

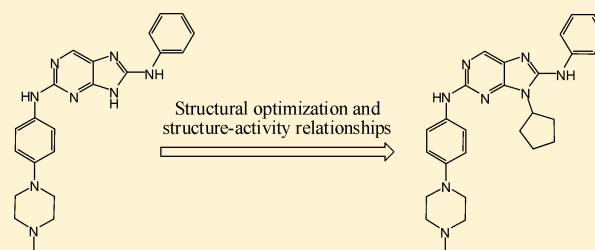
# Structural Optimization and Structure–Activity Relationships of $N^2$ -(4-(4-Methylpiperazin-1-yl)phenyl)- $N^8$ -phenyl-9*H*-purine-2,8-diamine Derivatives, a New Class of Reversible Kinase Inhibitors Targeting both EGFR-Activating and Resistance Mutations

Jiao Yang,<sup>†,‡,§</sup> Li-Jiao Wang,<sup>†,§</sup> Jing-Jing Liu,<sup>†</sup> Lei Zhong,<sup>†</sup> Ren-Lin Zheng,<sup>†</sup> Yong Xu,<sup>†</sup> Pan Ji,<sup>†</sup> Chun-Hui Zhang,<sup>†</sup> Wen-Jing Wang,<sup>†</sup> Xing-Dong Lin,<sup>†</sup> Lin-Li Li,<sup>‡</sup> Yu-Quan Wei,<sup>†</sup> and Sheng-Yong Yang<sup>\*,†</sup>

<sup>†</sup>State Key Laboratory of Biotherapy and Cancer Center, West China Hospital, West China Medical School, Sichuan University, Sichuan 610041, China

<sup>‡</sup>West China School of Pharmacy, Sichuan University, Sichuan 610041, China

**ABSTRACT:** This paper describe the structural optimization of a hit compound,  $N^2$ -(4-(4-methylpiperazin-1-yl)phenyl)- $N^8$ -phenyl-9*H*-purine-2,8-diamine (**1**), which is a reversible kinase inhibitor targeting both EGFR-activating and drug-resistance (T790M) mutations but has poor binding affinity. Structure–activity relationship studies led to the identification of 9-cyclopentyl- $N^2$ -(4-(4-methylpiperazin-1-yl)phenyl)- $N^8$ -phenyl-9*H*-purine-2,8-diamine (**9e**) that exhibits significant in vitro antitumor potency against the non-small-cell lung cancer (NSCLC) cell lines HCC827 and H1975, which harbor EGFR-activating and drug-resistance mutations, respectively. Compound **9e** was further assessed for potency and selectivity in enzymatic assays and in vivo anti-NSCLC studies. The results indicated that compound **9e** is a highly potent kinase inhibitor against both EGFR-activating and resistance mutations and has good kinase spectrum selectivity across the kinome. In vivo, oral administration of compound **9e** at a dose of 5 mg/kg caused rapid and complete tumor regression in a HCC827 xenograft model, and an oral dose of 50 mg/kg initiated a considerable antitumor effect in an H1975 xenograft model.



## 1. INTRODUCTION

Lung cancer has become the leading cause of cancer-related deaths worldwide.<sup>1</sup> More than 80% of all lung cancers are identified as non-small-cell lung cancer (NSCLC). The epidermal growth factor receptor (EGFR) has been established as one of the most important therapeutic targets for NSCLC.<sup>2,3</sup> Two small-molecule inhibitors of EGFR, gefitinib and erlotinib, have been approved by the U.S. Food and Drug Administration (FDA) for the treatment of NSCLC.<sup>4–6</sup> Both drugs can be classified as first-generation reversible, ATP-competitive inhibitors. Clinical studies indicate that NSCLC patients with EGFR-activating mutations, namely, exon 19 deletion or L858R mutations, benefit most from gefitinib/erlotinib treatment.<sup>7–9</sup> Unfortunately, NSCLCs with EGFR-activating mutations eventually develop resistance to these drugs, and in approximately half of these cases, resistance is caused by a single secondary mutation in the EGFR exon 20, resulting in a Thr-to-Met substitution at residue 790 (T790M).<sup>10–12</sup> A recent study by Yun and Eck indicated that the introduction of the T790 M mutation greatly increases the ATP binding affinity of the oncogenic activating mutant, hence reducing the potency of ATP-competitive kinase inhibitors.<sup>13</sup> Their study suggested that simply removing some of the steric hindrance from the current drugs is insufficient to restore potency to the T790 M mutant.

To overcome the enhanced ATP binding in T790 M mutants, the next-generation drug must bind to the T790 M mutant with higher affinity than that of the first-generation drugs. Irreversible EGFR inhibitors containing a Michael acceptor functional group have been developed to overcome this enhanced ATP binding by irreversibly alkylating a cysteine residue (C797) in the ATP binding site of the EGFR.<sup>14–21</sup> However, except for a few examples, such as BIBW2992,<sup>22</sup> PF00299804,<sup>23</sup> and WZ-4002,<sup>17</sup> these irreversible inhibitors have thus far shown limited clinical efficacy. Inherent weaknesses, including relatively high toxicity and a decreased binding velocity to the mutant kinase, may be responsible for the lack of clinical efficacy.<sup>24–26</sup> Hence, the development of next-generation reversible EGFR inhibitors that can inhibit the drug-resistant T790M-bearing mutants and remain potent in other activating mutants is a highly attractive goal that has received much attention in recent years.<sup>27–30</sup>

In an effort to discover inhibitors with novel scaffolds that are more potent against both EGFR-activating and resistance mutations, we performed a virtual screening against an in-house focused library containing approximately 650 000 known kinase

**Received:** September 21, 2012

**Published:** November 1, 2012

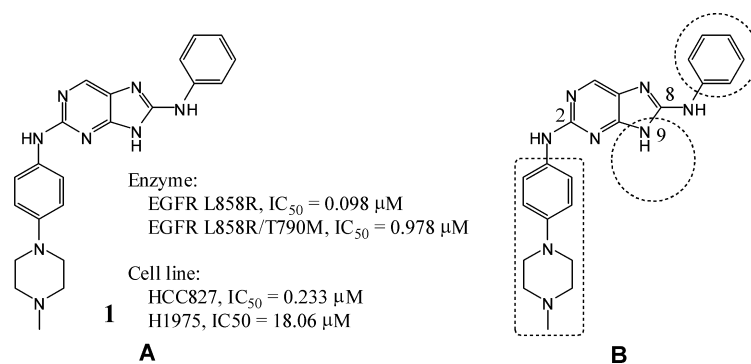
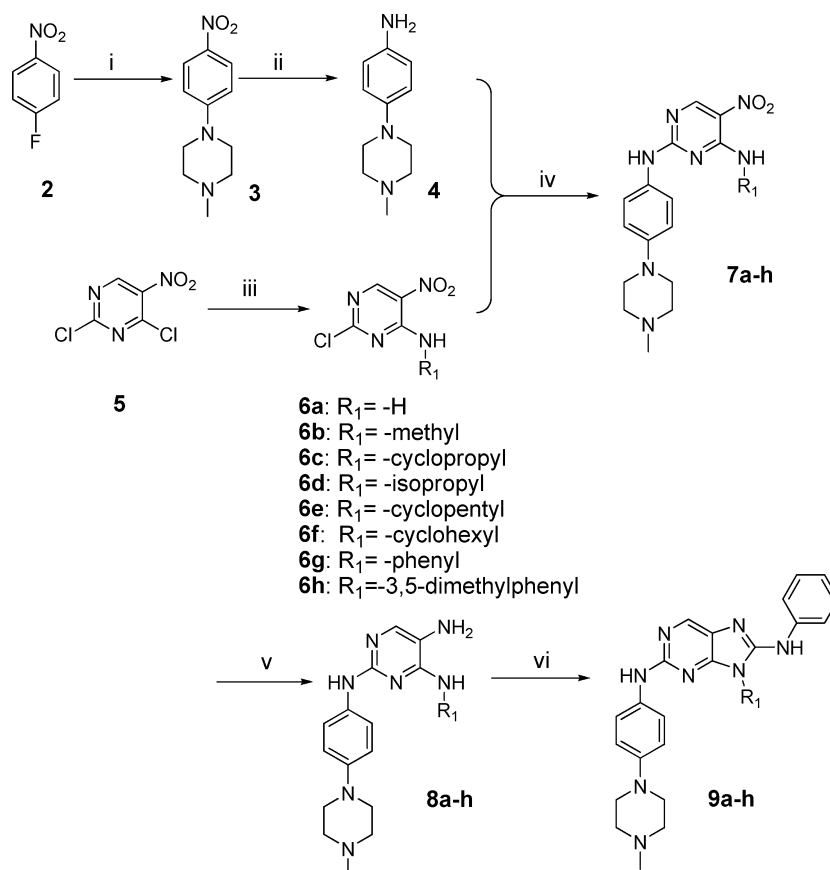


Figure 1. (A) Structure of hit compound 1. (B) Moieties in compound 1 targeted for modification in this study.

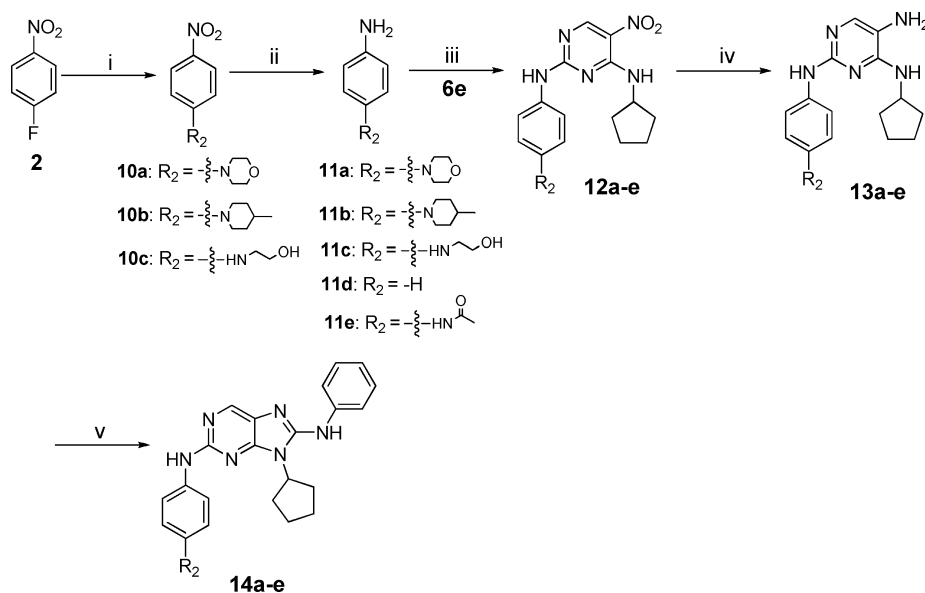
Scheme 1. Synthesis of 2,8-Dianilinopurine Derivatives 9a–g<sup>a</sup>



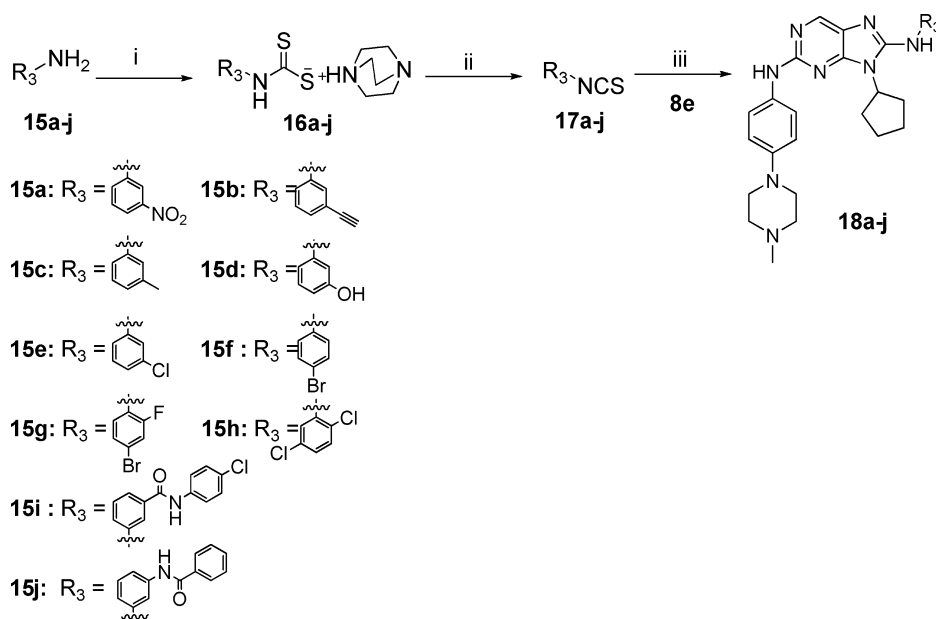
<sup>a</sup>Reagents and conditions: (i) 1-methylpiperazine,  $\text{K}_2\text{CO}_3$ , DMSO, rt, 6 h, 95%; (ii)  $\text{H}_2$ , 10% Pd/C, EtOH, rt, 9 h, 90%; (iii)  $\text{CH}_2\text{Cl}_2$ , DIEA, amine,  $-60^\circ\text{C}$  to room temperature, 60–75%; (iv) *n*-butanol,  $90^\circ\text{C}$ , 5 h, 76%; (v)  $\text{H}_2$ , 10% Pd/C, MeOH,  $50^\circ\text{C}$ , 6 h, 85%; (vi)  $\text{CH}_2\text{Cl}_2$ , DIEA, EDIC, isothiocyanatobenzene, reflux, 12 h, 35–60%.

inhibitors and kinase inhibitor-like compounds containing common kinase inhibitor core scaffolds (for details, see the Experimental Section). The virtual screen was followed by kinase inhibitory assays, which allowed us to find a hit compound, *N*<sup>2</sup>-(4-(4-methylpiperazin-1-yl)phenyl)-*N*<sup>8</sup>-phenyl-9*H*-purine-2,8-diamine (**1**, Figure 1A). This compound exhibits an ability to inhibit both EGFR-activating and resistance mutations; the  $IC_{50}$  values for the EGFR L858R and L858R/T790 M mutations are 0.098 and 0.978  $\mu\text{M}$ , respectively. In cellular assays, compound **1** displayed inhibitory activity against the gefitinib-sensitive NSCLC cell line HCC827 that bears the exon 19 deletion EGFR mutation (Del E746\_A750,  $IC_{50} = 0.233 \mu\text{M}$ ), but exhibited a weak inhibitory potency against the

gefitinib-resistant NSCLC cell line H1975 that harbors the L858R/T790 M EGFR mutation ( $IC_{50} = 18.06 \mu\text{M}$ ). Although compound **1** has some ability to inhibit both EGFR-activating and resistance mutations, the potencies are insufficient. In particular, the relatively poor potency against the T790 M EGFR mutation indicates that it cannot overcome the enhanced ATP binding found in T790 M EGFR. Our goal in this study was to optimize the structure of compound **1** and derive compounds with higher potency that can inhibit the drug-resistant T790M-bearing mutants while remaining potent in the presence of the activating mutations. A series of novel 2,8-dianilinopurine derivatives were synthesized and tested for bioactivity. The most potent derivative, compound **9e**, was then

Scheme 2. Synthesis of 2,8-Dianilino-9-cyclopentylpurine Derivatives 14a–e<sup>a</sup>

<sup>a</sup>Reagents and conditions: (i) morpholine, 4-methylpiperidine, ethanolamine, K<sub>2</sub>CO<sub>3</sub>, DMSO, rt, 6 h, 70–85%; (ii) H<sub>2</sub>, 10% Pd/C, EtOH, rt, 9 h, 90%; (iii) *n*-butanol, 90 °C, 5 h, 76%; (iv) H<sub>2</sub>, 10% Pd/C, MeOH, 50 °C, 6 h, 85%; (v) CH<sub>2</sub>Cl<sub>2</sub>, DIEA, EDIC, isothiocyanatobenzene, reflux, 12 h, 35–60%.

Scheme 3. Synthesis of 2,8-Dianilino-9-cyclopentylpurine Derivatives 18a–j<sup>a</sup>

<sup>a</sup>Reagents and conditions: (i) EtOH, CS<sub>2</sub>, DABCO, rt, 12 h, 60%; (ii) CH<sub>2</sub>Cl<sub>2</sub>, triphosgene, 0 °C, 1 h, reflux, 4 h, 65%; (iii) CH<sub>2</sub>Cl<sub>2</sub>, DIEA, EDIC, reflux, 12 h, 35–60%.

subjected to further evaluation of its antitumor activities both in vitro and in vivo. We report the chemical synthesis and structure–activity relationships (SARs) between this novel series of compounds and the in vitro and in vivo anti-NSCLC activities of compound **9e**.

## 2. RESULTS AND DISCUSSION

### 2.1. Synthesis of 2,8-Dianilino-9-cyclopentylpurine Derivatives.

Structural optimization was carried out by focusing on the N-9 (H), C-2 (anilino group), and C-8 positions (anilino group) of the purine scaffold (Figure 1B). Scheme 1 depicts the

synthetic route to the 2,8-dianilino-9-cyclopentylpurine derivatives **9a–h** in which the N-9 (H) position of the purine scaffold is substituted by various groups. Commercially available 4-fluoronitrobenzene (**2**) reacted with 1-methylpiperazine in the presence of K<sub>2</sub>CO<sub>3</sub> in DMSO to produce the intermediate **3**. The catalytic hydrogenation of the nitro functionality in **3** with palladium on carbon (Pd/C) provided the desired aniline **4** in excellent yield. Reaction of the commercially available 2,4-dichloro-5-nitropyrimidine (**5**) with various amines, including ammonia, methanamine, cyclopropanamine, propan-2-amine, cyclopentylamine, cyclohexylamine, aniline, and 3,5-dimethylaniline,

produced intermediates **6a–h**. Nucleophilic aromatic substitution of the 2-chloro position in **6a–h** with **4** in *n*-butanol at 90 °C yielded compounds **7a–h**. Subsequent hydrogenation of the nitro group in **7a–h** using Pd/C as a catalyst provided a good yield of the desired intermediates **8a–h**, which were treated with isothiocyanatobenzene to produce the final 2,8-dianilino-purine derivatives **9a–h**.

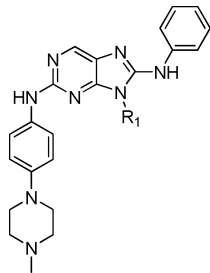
Scheme 2 shows a general route for the synthesis of 2,8-dianilino-9-cyclopentylpurine derivatives **14a–e** bearing different substituents on the phenyl ring of the 2-anilino group. The fluorine in 4-fluoronitrobenzene was substituted via conventional nucleophilic aromatic substitution using morpholine, 4-methylpiperidine, and ethanolamine in the presence of K<sub>2</sub>CO<sub>3</sub> in DMSO to yield the corresponding substituted nitrobenzenes **10a**, **10b**, and **10c**, respectively. As before, the nitro functional groups in compounds **10a–c** were reduced via catalytic hydrogenation to generate the corresponding anilines **11a–c** in high yield. These intermediates, **11a–c**, along with the commercially available compounds **11d** and **11e** were treated with compound **6e** in *n*-butanol at 90 °C to produce **12a–e**. These compounds were then hydrogenated with catalytic Pd/C, and the resultant intermediates (**13a–e**) were treated with isothiocyanatobenzene to yield the final 2,8-dianilino-9-cyclopentylpurine derivatives **14a–e**.


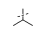
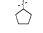
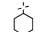
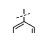
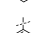
Scheme 3 depicts the synthetic route to 2,8-dianilino-9-cyclopentylpurine derivatives **18a–j** with different substituents on the phenyl ring of the 8-anilino group. Substituted anilines **15a–j** reacted with CS<sub>2</sub> and DABCO in ethanol at room temperature to yield the intermediate compounds **16a–j**, which were directly treated with triphosgene at 35–40 °C in dichloromethane to produce substituted phenyl isothiocyanates **17a–j** with yields of 45–60%. Compounds **17a–j** were treated with compound **8e** and EDCI in the presence of *N,N*-diisopropylamine in dichloromethane to yield the final 2,8-dianilino-9-cyclopentylpurine derivatives **18a–j** in acceptable yields.

**2.2. SAR of 2,8-Dianilino-purine Derivatives.** Cell-based assays were used to evaluate the bioactivity of the synthesized compounds in the SAR studies. Two human NSCLC cell lines, HCC827 and H1975, and a human hepatocellular carcinoma cell line, HepG2, were used in the study. These cell lines were selected for several reasons: The HCC827 cell line harbors an EGFR-activating mutation (deletion mutation) and is a representative EGFR-driven cell line. The H1975 cell line bears the drug resistance mutation in EGFR (L858R/T790M) and is a typical EGFR-driven cell line. Clearly, these two cell lines are suitable for studies seeking inhibitors of EGFR-activating and resistant mutants. The use of HepG2, which harbors wild-type EGFR and is not dependent on EGFR signaling for cell growth, is used to rule out activity due to non-EGFR-mediated effects (“off target” or cellular toxicity effects). The SAR obtained from such cell-based assays potentially reports a combination of the intrinsic activity of the compounds against the kinase target and the ability of the compounds to permeate the cell membrane during the assay. The enzymatic binding affinities of the inhibitors with the highest potency at the cellular level were also measured. The most potent compound in both the enzymatic and cellular assays was selected for *in vivo* experiments to evaluate its activity against NSCLC. Another advantage of using cell-based assays in the SAR studies is their reduced cost relative to enzymatic assays, which is especially meaningful in an academic setting.

**2.2.1. Substitution Effects at the N-9 Position of the Purine.** To explore the effect of substitution at the N-9 position of the purine scaffold, we synthesized compounds **9a–h** (Scheme 1), which contain hydrophobic substituents of different sizes at the N-9 purine position. The antiviability activities of compounds **9a–h** against the HCC827, H1975, and HepG2 cell lines are shown in Table 1. Introduction of a

**Table 1.** 2,8-Dianilino-purine Derivatives Containing Different Substituents at the N-9 Position of the Purine Scaffold and Their Antiviability Activities against HCC827, H1975, and HepG2 Cells<sup>a</sup>



Compound	R <sub>1</sub>	HCC827 <sup>a</sup> (IC <sub>50</sub> , μM)	H1975 <sup>a</sup> (IC <sub>50</sub> , μM)	HepG2 (IC <sub>50</sub> , μM)
<b>9a</b>	-H	0.233±0.051	18.06±2.56	>5
<b>9b</b>	-CH <sub>3</sub>	0.024±0.005	6.06±1.05	>5
<b>9c</b>		0.018±0.004	2.86±0.34	>5
<b>9d</b>		0.0001±0.000025	0.96±0.029	>5
<b>9e</b>		<0.00001	0.36±0.033	>5
<b>9f</b>		<0.00001	0.39±0.011	>5
<b>9g</b>		0.0017±0.00034	1.83±0.38	>5
<b>9h</b>		0.001±0.0003	1.91±0.47	>5

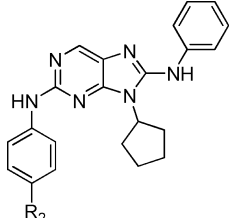
<sup>a</sup>Each compound was tested in triplicate; the data are presented as the mean ± SD.

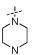
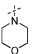
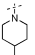
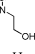
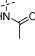
methyl group (**9b**) at the N-9 position of the purine increases its antiviability activity against both H1975 and HCC827. Substitution with bulkier cyclopropyl (**9c**) and isopropyl (**9d**) groups, which both contain three carbon atoms, further increases the antiviability activity against both the H1975 and HCC827 cell lines. Increasing the substituent size to cyclopentyl yields compound **9e**, which has an inhibitory potency (IC<sub>50</sub>) of 0.36 μM against H1975 and <0.00001 μM against HCC827. However, further increases in the substituent size (e.g., cyclohexyl (**9f**), phenyl (**9g**), or 3,5-dimethylbenzene (**9h**)) do not cause an increase in the bioactivity. On the contrary, these larger substituents lead to decreased bioactivity relative to cyclopentyl (**9e**), implying that cyclopentyl represents the optimum substituent size at the N-9 position. Additionally, most of these compounds have IC<sub>50</sub> values of >5 μM against the HepG2 cell line, indicating that the antiviability activity of compound **9e** against the HCC827 and H1975 cell lines is not due to cellular toxicity (the same situation will be seen below).

**2.2.2. Substitution on the Phenyl Ring of the 2-Anilino Group.** We investigated the possible influence that substituents on the benzene ring of the 2-anilino group have on bioactivity. For this purpose, the N-9 cyclopentyl group and the C-8 anilino group were held constant. The leading derivatives, **14a–**

e and 9e, are shown in Table 2 with the corresponding bioactivity data. The different substituents on the benzene ring

**Table 2. Compounds 9e and 14a–c Containing Different Substituents on the Benzene Ring of the 2-Anilino Group of the Purine Scaffold and Their Antiviability Activity against HCC827, H1975, and HepG2 Cells<sup>a</sup>**



Compound	R <sub>2</sub>	HCC827 <sup>a</sup> (IC <sub>50</sub> , μM)	H1975 <sup>a</sup> (IC <sub>50</sub> , μM)	HepG2 <sup>a</sup> (IC <sub>50</sub> , μM)
9e		<0.00001	0.36±0.033	>5
14a		0.00066±0.000045	9.2±0.12	>5
14b		0.032±0.0062	9.8±0.11	>5
14c		0.0028±0.00038	2.81±0.27	>5
14d	-H	0.0027±0.00041	>10	>5
14e		0.00047±0.000012	1.21±0.34	>5

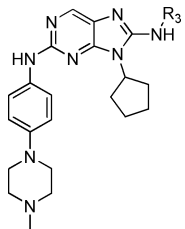
<sup>a</sup>Each compound was tested in triplicate; the data are presented as the mean ± SD.

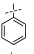
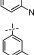
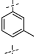
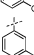
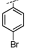
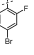
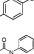
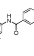



of the 2-anilino group have considerable influence on the antiviability activity against both H1975 and HCC827. However, compound 9e remains the most active compound. Compound 9e possesses a 4-methylpiperazine substituent, which is the most polar group explored at that position.

**2.2.3. Substitution on the Phenyl Ring of the 8-Anilino Group.** We also examined the impact on bioactivity of the substitution onto the phenyl ring of the 8-anilino group. The N-2 and C-9 positions were held constant as 1-methyl-4-phenylpiperazine and cyclopentyl moieties, respectively. Substitution was introduced at the meta-, ortho-, and/or para-positions of the phenyl ring of the 8-anilino group. The best performing compounds, 18a–j and 9e, and their antiviability activity against the H1975, HCC827 and HepG2 cell lines are shown in Table 3. Substitution of the 8-anilino group onto the phenyl ring reduced the antiviability activity against the HCC827 and H1975 cell lines, although the bioactivity against the HCC827 cell line was maintained at a picomolar level for most of the derivatives.

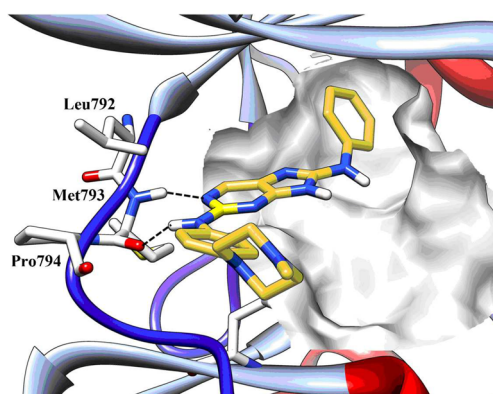
**2.3. Rationalization of the Observed SAR Using Molecular Docking.** The observed SAR demonstrates that a substituent of suitable size at the N-9 position of the purine scaffold can increase the binding affinity. Substitutions of the 2-anilino and 8-anilino groups onto the phenyl ring did not increase the bioactivity. To rationalize the observed SAR, molecular docking studies were performed. The binding mode of compound 1 within the active site of the T790 M EGFR mutant predicted by molecular docking is shown in Figure 2. The purine ring is located in the ATP-binding pocket and is sandwiched between the N- and C-lobes of the kinase. The

**Table 3. Compound 9e and 2,8-Dianilino-9-cyclopentylpurine Derivatives 18a–j Containing Substituents on the Phenyl Ring of the 8-Anilino Group and Their Antiviability Activity against HCC827, H1975, and HepG2 Cells<sup>a</sup>**



Compound	R <sup>3</sup>	HCC827 <sup>a</sup> (IC <sub>50</sub> , μM)	H1975 <sup>a</sup> (IC <sub>50</sub> , μM)	HepG2 <sup>a</sup> (IC <sub>50</sub> , μM)
9e		<0.00001	0.36±0.033	>5
18a		<0.00001	0.98±0.086	>5
18b		<0.00001	0.65±0.088	4.9±0.42
18c		<0.00001	0.56±0.063	4.7±0.36
18d		0.00072±0.000027	1.02±0.21	4.2±0.19
18e		<0.00001	0.39±0.067	4.8±0.32
18f		0.0022±0.00031	2.09±0.27	>5
18g		0.0023±0.00056	1.12±0.19	>5
18h		<0.00001	2.54±0.46	>5
18i		2.9±0.48	4.01±0.29	>5
18j		0.015±0.0042	2.12±0.75	2.6±0.22

<sup>a</sup>Each compound was tested in triplicate; the data are presented as the mean ± SD.



**Figure 2.** Putative binding mode of compound 1 within the active pocket of the EGFR T790 M mutant (the EGFR T790 M structure was taken from PDB 2J1U). Hydrogen bonds are shown as black dashed lines.

molecule is oriented such that the 2-anilino branch extends toward the solvent and the 8-anilino moiety is directed into the back of the ATP-binding pocket. Two highly conserved hydrogen bonds are formed between compound 1 and the “hinge” region that links the N- and C-lobes of the kinase. The binding mode of compound 1 also reveals that a hydrophobic

region near the N-9 position of the purine, which is normally occupied by the ribose moiety of ATP, remains unoccupied. A hydrophobic substituent on the N-9 position of the purine should be preferred and is expected to increase the binding affinity. This prediction is consistent with the previously observed SAR; substitutions at the N-9 position of the purine considerably increased the bioactivity. However, a substituent that is too large may become unfavorable given the limited size of the hydrophobic pocket. This prediction is also consistent with our observations that larger substituents (e.g., cyclohexyl, phenyl, and 3,5-dimethylphenyl) led to a decrease in the potency in comparison with the cyclopentyl group. In contrast, the 2-aniline branch of this molecule extends toward the solvent, and the polar 1-methylpiperazine group seems favorable at this position. The 8-anilino group is located in the back of ATP-binding pocket. Substitution on the phenyl ring of 8-aniline is not preferred, which is consistent with possible collisions between the substituent and the residues in the back of ATP-binding pocket.

**2.4. Binding Affinities of Compound 9e to Various EGFR Mutations.** The structural optimization and SAR studies beginning with compound 1 resulted in the discovery of compound 9e, which is the most active compound of the analogues tested. The potency and selectivity of compound 9e were further examined through enzymatic assays.

The binding affinities ( $K_d$  values) of compound 9e to various EGFR mutations including activating and drug-resistance mutations were measured using KINOMEscan kinase binding assays (Ambit Biosciences), and the results are presented in Table 4. Compound 9e has a picomolar binding affinity with

**Table 4. Binding Affinities of Compound 9e to Various EGFR Mutations**

kinase	$K_d$ ( $\mu\text{M}$ )
EGFR (WT)	0.0006
EGFR (E746-A750del)	0.0005
EGFR (747-E749del, A750P)	0.0004
EGFR (L747-S752del, Sins)	0.0005
EGFR (L858R)	0.0006
EGFR (G719C)	0.0007
EGFR (G719S)	0.0005
EGFR (L861Q)	0.0006
EGFR (L858R, T790M)	0.0016

wild-type (WT) EGFR (0.0006  $\mu\text{M}$ ) and various EGFR-activating mutations, including EGFR (E746-A750del) ( $IC_{50}$  = 0.0005  $\mu\text{M}$ ), EGFR (L747-E749del, A750P) ( $IC_{50}$  = 0.0004  $\mu\text{M}$ ), EGFR (L747-S752del, Sins) ( $IC_{50}$  = 0.0005  $\mu\text{M}$ ), EGFR (L858R) ( $IC_{50}$  = 0.0006  $\mu\text{M}$ ), EGFR (G719C) ( $IC_{50}$  = 0.0007  $\mu\text{M}$ ), EGFR (G719S) ( $IC_{50}$  = 0.0005  $\mu\text{M}$ ), and EGFR (L861Q) ( $IC_{50}$  = 0.0006  $\mu\text{M}$ ). It also exhibited picomolar binding affinity to the drug-resistant T790 M EGFR mutant (L858R, T790M) ( $IC_{50}$  = 0.0016  $\mu\text{M}$ ).

**2.5. Kinase Inhibition Profile for Compound 9e against Recombinant Human Protein Kinases.** The kinase inhibition profile for compound 9e against a panel of recombinant human protein kinases was measured using the “gold standard” radiometric kinase assay, and the results are shown in Table 5. Compound 9e was a potent inhibitor of EGFR(WT) with an  $IC_{50}$  value of 0.004  $\mu\text{M}$ . It also inhibited several other oncokines including ERBB2, ERBB4, KIT, SRC, SYK, and p38 $\alpha$  with moderate potencies ( $IC_{50}$  = 0.06, 0.03,

**Table 5. Kinase Inhibition Profile for Compound 9e against Human EGFR and a Panel of Other Selected Protein Kinases**

kinase	$IC_{50}$ ( $\mu\text{M}$ )	kinase	$IC_{50}$ ( $\mu\text{M}$ )
CDK2	>10	JNK2	1.5
ALK	2.3	MK2	>10
EGFR	0.004	MK5	>10
ERBB2	0.06	MNK1	6.7
ERBB4	0.03	MNK2	3.2
IGF1R	>10	PDK1	>10
INSR	>10	PIM2	>10
KIT	0.54	PKA	1.1
MET	6.4	PKBa	>10
MST1R	>10	PKC $\alpha$	6.7
SRC	0.29	PKC $\theta$	3.6
SYK	0.72	PKN1	6.1
CK1	>10	PKN2	>10
COT1	>10	PLK1	>10
CaMK2	>10	ROCK2	>10
ERK2	>10	S6K	9.4
GSK3 $\beta$	>10	TYK2	6.7
IRAK4	>10	VEGFR2	0.02
JAK1	3.3	WNK1	>10
JAK2	1.2	p38 $\alpha$	0.23
JAK3	2.6	p38 $\gamma$	>10

0.54, 0.29, 0.72, and 0.23  $\mu\text{M}$ , respectively), but only weakly inhibited ALK, MET, JAK1, JAK2, JAK3, JNK2, MNK1, MNK2, PKA, PKC $\alpha$ , PKC $\theta$ , PKN1, S6K, and TYK2 ( $IC_{50}$  = 2.3, 6.4, 3.3, 1.2, 2.6, 1.5, 6.7, 3.2, 1.1, 6.7, 3.6, 6.1, 9.4, and 6.7  $\mu\text{M}$ , respectively). Compound 9e displayed almost no inhibitory activity in 20 other protein kinases. These data demonstrate that compound 9e is a potent EGFR inhibitor with good kinase spectrum selectivity, although it also exhibits considerable potency against several other oncokines.

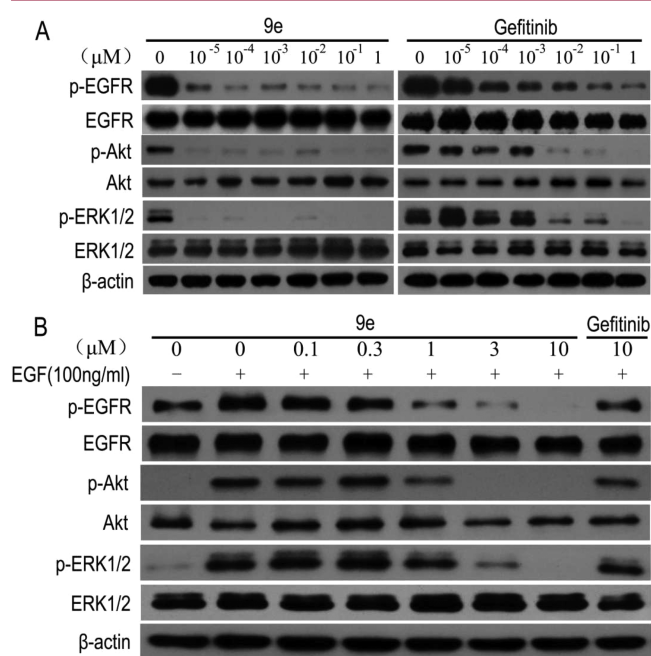
**2.6. In Vitro Antiviability Activity of Compound 9e.** The antiviability potency of compound 9e against various tumor cell lines was measured using the MTT assay method (Table 6). Compound 9e displayed exceptional potency against NSCLC cell lines HCC827 and PC-9 (del E746\_A750) with

**Table 6. Antiviability Activities of Compound 9e and Gefitinib against Various Cancer Cell Lines ( $IC_{50}$ ,  $\mu\text{M}$ )**

cancer type	cell line	characteristic	compound 9e	gefitinib
NSCLC	HCC827	Del E746_A750 (EGFR mutant)	<0.00001	0.0015
NSCLC	PC-9	Del E746_A750 (EGFR mutant)	0.00022	0.014
NSCLC	H1975	L858R/T790 M (EGFR mutant)	0.36	~10
NSCLC	Calu-3	ErbB2 overexpressed	0.12	1.6
NSCLC	H292	EGFR overexpressed	0.045	0.12
epidermal	A431	EGFR overexpressed	0.12	4
hypopharyngeal	Fadu	EGFR overexpressed	0.015	0.05
breast	MDA-MB-231	KRAS mutation (G13D)	5	>10
colon	HCT116	KRAS and PI3k mutations	3	>10
liver	HepG2	EGFR independent	>5	>10

IC<sub>50</sub> values of <0.00001 and 0.00022  $\mu$ M, respectively, and was much more potent than gefitinib (0.0015 and 0.014  $\mu$ M, respectively; see Table 6). In the drug-resistant NSCLC cell line H1975, compound **9e** also exhibited good inhibition potency with an IC<sub>50</sub> value of 0.36  $\mu$ M. In cell lines in which EGFR is overexpressed, including Calu-3, H292, A431, and FaDu, compound **9e** displayed higher inhibition potency than gefitinib. In other cell lines, including MDA-MB-231, HCT116, and HepG2, which bear a lower EGFR expression or present cell growth that is not dependent on EGFR, compound **9e** exhibited little or no inhibition potency. These results demonstrate the good cellular selectivity of compound **9e**.

**2.7. Inhibition of EGFR Autophosphorylation and the Inactivation of Downstream Signaling Proteins in Cell Cultures.** The ability of compound **9e** to inhibit the activation of EGFR and the downstream signaling proteins with which it interacts were assessed using Western blot analysis, and the results are presented in Figure 3. In the HCC827 cell line,



**Figure 3.** Inhibition of EGFR autophosphorylation and inactivation of downstream signaling proteins in cell cultures by compound **9e**. (A) HCC827 cells were treated with compound **9e** or gefitinib for 8 h. The cells were lysed, and the proteins were assessed by Western blot assay. (B) Serum-starved H1975 cells were treated with compound **9e** or gefitinib for 3 h, followed by the addition of EGF (100 ng/mL) for 15 min. Protein extracts were then analyzed by Western blot assay.

compound **9e** inhibited EGFR phosphorylation at a low concentration (<0.00001  $\mu$ M) and down-regulated the phosphorylation of the downstream signaling proteins, AKT and the extracellular signal-regulated kinase (ERK). This effect was more pronounced with compound **9e** than with gefitinib. In the EGF-stimulated H1975 cell line, compound **9e** inhibited EGF-dependent phosphorylation of EGFR and the downstream signaling proteins AKT and ERK in a dose-dependent manner with an estimated IC<sub>50</sub> value of 0.4  $\mu$ M. However, the EGFR signaling pathway was not inhibited by gefitinib at a concentration of 10  $\mu$ M.

**2.8. In Vivo Anti-NSCLC Effects of Compound 9e.** The in vivo anti-NSCLC effects of compound **9e** were evaluated using HCC827 and H1975 tumor xenograft models. In the

HCC827 tumor model, the mice were treated via oral gavage once daily with either compound **9e** or gefitinib once the tumor had grown to a volume of 300–500 mm<sup>3</sup>. At all doses tested, compound **9e** markedly inhibited the tumor growth, and a 5 mg/kg/day dose of compound **9e** resulted in complete tumor regression within 15 days of treatment (see Figure 4A). Similar results were observed with gefitinib at a dose of 100 mg/kg/day. Moreover, at the dose of 1 mg/kg/day, compound **9e** displayed better antitumor activity than gefitinib.

In the H1975 tumor model, established sc tumors with volumes of 50–100 mm<sup>3</sup> were treated with compound **9e**. Oral administrations of the compound at 25 and 50 mg/kg/day inhibited tumor growth in a dose-dependent manner at rates of 35 and 62%, respectively (see Figure 4B). Treatment with gefitinib at 100 mg/kg produced only a marginal effect on tumor growth (23% inhibition, data not shown). BIBW2992 (an irreversible EGFR inhibitor) was used as a positive control and had an inhibition rate of 74% at a dose of 20 mg/kg/day. During the experiment, only minor weight loss was observed in the high-dose groups (compound **9e**, 4.4% at 50 mg/kg; BIBW2992, 6.6% at 20 mg/kg), which was recovered with continued treatment.

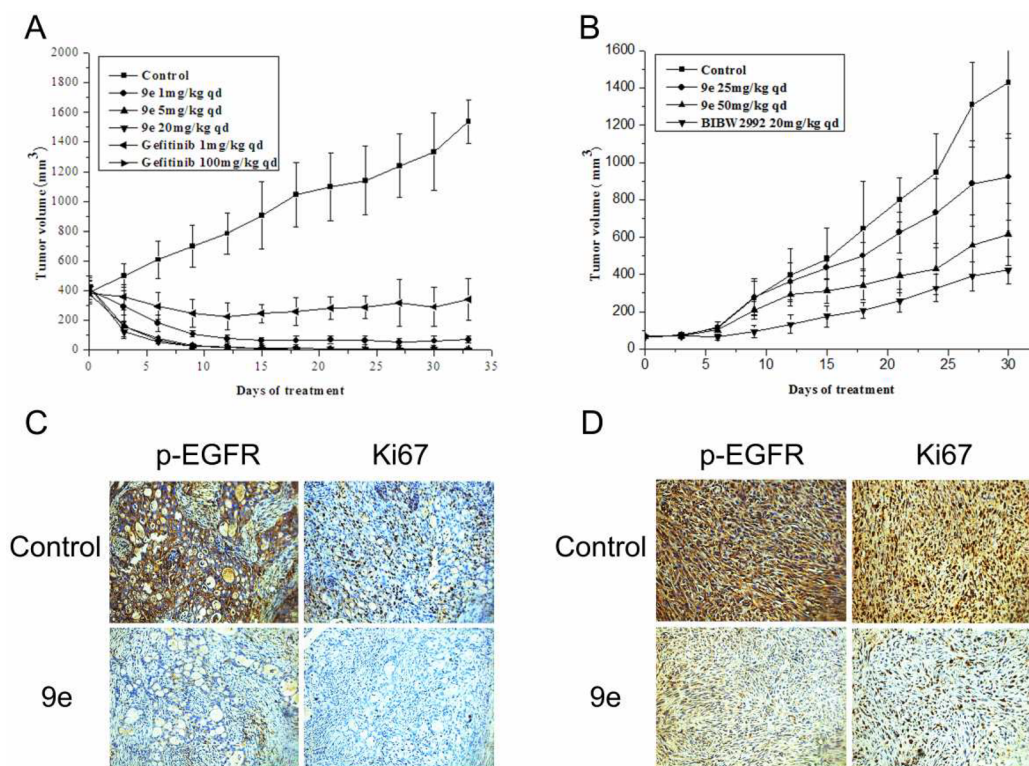
The ability of compound **9e** to inhibit EGFR phosphorylation and cell proliferation (Ki67) in tumor tissues was also evaluated using histological and immunohistochemical techniques (Figure 4C,D). In the HCC827 model, a 1 mg/kg/day dose of compound **9e** was administered, and after treatment for 3 days, the tumors were collected and analyzed. In the H1975 model, a dose of 50 mg/kg/day was administered, and tumors were collected and analyzed after 10 days of treatment. In both models, significant decreases were observed in the staining of EGFR phosphorylation and Ki67 for those groups treated with compound **9e** as compared with the control groups. These findings indicate that compound **9e** significantly inhibited the EGFR phosphorylation and reduced the proliferation ability of the tumor cells.

### 2.9. Pharmacokinetic Characteristics of Compound 9e

The pharmacokinetic parameters of compound **9e** following per os administration in male rats are summarized in Table 7. After oral administration at a single dose of 20 mg/kg, compound **9e** displayed a CL of 9.72 L/h/kg with a moderate  $t_{1/2}$  of 4.86 h. The steady-state volume ( $V_{ss} = 63.35$  L/kg) was much larger than the volume of total body water, suggesting extravascular distribution. Moreover, the absorption of compound **9e** was relatively quick and reached a maximum plasma concentration ( $C_{max} = 0.23$  mg/L) in 1–3 h.

## 3. CONCLUSIONS

We have described the structural optimization of a hit compound, *N*<sup>2</sup>-(4-(4-methylpiperazin-1-yl)phenyl)-*N*<sup>8</sup>-phenyl-9*H*-purine-2,8-diamine (**1**), which exhibited poor binding affinity ( $K_d$ ) for both EGFR-activating and drug-resistant mutants. SAR studies centering around the *N*-9 (H), *C*-2 (anilino), and *C*-8 (anilino) groups of the purine scaffold led to the discovery of compound **9e**. This compound exhibited significantly increased antiviability potency against the HCC827 cell line, which harbors an activating mutation in EGFR, and the H1975 cell line, which contains the drug-resistance EGFR mutation T790M. Compound **9e** displayed only weak inhibition against HepG2, a cell line that is not EGFR-driven. Further in vitro assays indicated that compound **9e** has a high potency against both EGFR-activating and drug-resistant EGFR mutants and good kinase spectrum selectivity, while also



**Figure 4.** In vivo antitumor effects of compound **9e** and its action mechanism. (A) Tumor growth curves for the HCC827 xenograft model. (B) Tumor growth curves for the H1975 xenograft model. Animals were randomized into groups ( $n = 6-8/\text{group}$ ) and administered compound **9e**, gefitinib, BIBW2992, or vehicle once daily at the indicated dose levels when tumors reached the determined size. In both models, the animal weight and tumor volume were monitored twice weekly. Points indicate mean tumor volume ( $\text{mm}^3$ ); bars indicate SD. (C, D) Histological and immunohistochemical analyses demonstrating the effects of compound **9e** on the inhibition of EGFR phosphorylation and cell proliferation (Ki67) in tumor tissues. (C) In the HCC827 model, a dose of 1 mg/kg/day of compound **9e** was administered. After treatment for 3 days, the tumors were collected and analyzed. (D) In the H1975 model, a dose of 50 mg/kg/day was administered, and the tumors were collected and analyzed after 10 days of treatment.

**Table 7. Pharmacokinetic Parameters for Compound 9e in Plasma after the Oral Administration of a 20 mg/kg Dose to Sprague–Dawley Rats**

parameter	po (20 mg/kg)
AUC <sub>(0-24h)</sub> (mg/L × h)	2.14
$t_{1/2}$ (h)	4.86
$T_{\text{max}}$ (h)	1–3
$V_{\text{ss}}$ (L/kg)	63.35
CL (L/h/kg)	9.72
$C_{\text{max}}$ (mg/L)	0.23

inhibiting several other oncokinasases. Western blot analysis showed that compound **9e** significantly inhibited EGFR phosphorylation and the activation of downstream signaling proteins. In vivo antitumor activity assays showed that an oral, once-daily dose of compound **9e** at 5 mg/kg for 15 days led to complete tumor regression in the HCC827 xenograft model and that a once-daily dose of compound **9e** at 50 mg/kg exhibited considerable tumor inhibition in the H1975 xenograft model. Preliminary pharmacokinetic studies indicated that compound **9e** possesses good pharmacokinetic properties. Because compound **9e** is a multikinase inhibitor, synergistic effects from the simultaneous inhibition of EGFR and other kinases are possible. Further detailed studies of the action mechanisms of compound **9e** are underway and will be reported elsewhere.

#### 4. EXPERIMENTAL SECTION

**Chemistry Methods.** Unless otherwise noted, all materials were obtained from commercial suppliers and used without further purification. The syntheses of compounds **9a–g**, **14a–e**, and **18a–j** were as previously reported. The purity of all final compounds was determined by high-performance liquid chromatography (HPLC) analysis to be >95%. HPLC analysis was carried out on a Waters 2695 HPLC system with the use of a Kromasil C18 column (4.6 mm × 250 mm, 5 $\mu\text{m}$ ). <sup>1</sup>H NMR spectra were recorded on a Bruker AV-400 spectrometer at 400 MHz. Chemical shifts ( $\delta$ ) are expressed in parts per million (ppm) with TMS as an internal standard. Multiplicities are given as s (singlet), d (doublet), dd (double-doublet), t (triplet), q (quartet), m (multiplet), and br (broad signal). MS spectral data were obtained on an Agilent 1100 series with UV detection at 254 nm using electrospray ionization. Thin layer chromatography (TLC) was conducted on aluminum sheet silica gel Merck 60F254. The spots were visualized using ultraviolet light.

**1-Methyl-4-(4-nitrophenyl)piperazine (3).** A solution of 4-fluoronitrobenzene (10 g, 70.9 mmol), and K<sub>2</sub>CO<sub>3</sub> (10.76 g, 78.1 mmol) in DMSO (15 mL) was stirred at room temperature for 0.5 h. Subsequently, 1-methylpiperazine (8 mL, 70.9 mmol) was added dropwise, and the resulting reaction mixture was stirred at room temperature for 6 h. The mixture was then poured into ice–water. A yellow precipitate formed and was collected by filtration to give **3** (13.3 g, 85% yield, 98%



HPLC purity):  $^1\text{H NMR}$  (400 MHz,  $\text{DMSO-}d_6$ ),  $\delta$  8.04 (d,  $J = 8.0$  Hz, 2H), 7.02 (d,  $J = 8.0$  Hz, 2H), 3.44 (t,  $J = 6.0$  Hz, 4H), 2.51 (t,  $J = 6.0$  Hz, 4H), 2.12 (s, 3H); MS (ESI, positive ion),  $m/z$  222.41 [ $\text{M} + \text{H}$ ] $^+$ .

**4-(4-Methylpiperazin-1-yl)phenylamine (4).** Compound 3 (5 g, 22.6 mmol) was dissolved in ethanol (150 mL), and to this solution was added 10% Pd/C (0.5 g). The reaction mixture was stirred at room temperature under an atmosphere of  $\text{H}_2$  for 9 h. After completion of the reaction, the resulting mixture was filtered through Celite, and the filtered catalyst was washed with ethanol. The filtrate was concentrated under high vacuum to afford compound 4 as a fuchsia solid (3.6 g, 85% yield, 96% HPLC purity):  $^1\text{H NMR}$  (400 MHz,  $\text{DMSO-}d_6$ ),  $\delta$  6.67 (d,  $J = 8.8$  Hz, 2H), 6.48 (d,  $J = 8.8$  Hz, 2H), 4.52 (s, 2H), 2.89–2.87 (m, 4H), 2.50–2.48 (m, 4H), 2.19 (s, 3H); MS (ESI, positive ion),  $m/z$  192.41 [ $\text{M} + \text{H}$ ] $^+$ .

**2-Chloro-5-nitropyrimidin-4-amine (6a).** 2,4-Dichloro-5-nitropyrimidine (5 g, 26 mmol) and DIEA (4.7 mL, 30.9 mmol) were dissolved in  $\text{CH}_2\text{Cl}_2$  (300 mL) and cooled to  $-60$  °C. Ammonium hydroxide (3.0 mL, 78 mmol) was added dropwise. The reaction mixture was stirred at  $-60$  °C for about 1 h. Then the cooling bath was removed, and the reaction mixture was stirred at room temperature for about 0.5 h. A yellow precipitate formed and was collected by filtration, rinsing with EtOH, to give compound 6a (4 g, 90% yield, 95% HPLC purity):  $^1\text{H NMR}$  (400 MHz,  $\text{DMSO-}d_6$ ),  $\delta$  9.20 (s, 1H), 9.02 (s, 1H), 8.60 (s, 1H); MS (ESI, positive ion),  $m/z$  175.8 [ $\text{M} + \text{H}$ ] $^+$ .

**General Procedure for the Preparation of the Compounds 6b–e.** 2-Chloro-*N*-methyl-5-nitropyrimidin-4-amine (6b). 2,4-Dichloro-5-nitropyrimidine (5 g, 26 mmol) and DIEA (4.7 mL, 30.9 mmol) were dissolved in  $\text{CH}_2\text{Cl}_2$  (300 mL) and cooled to  $-60$  °C. A solution of methylamine (1.2 mL, 28.6 mmol) in water was added dropwise. The reaction mixture was stirred at  $-60$  °C for about 1 h. TLC showed that the reaction is complete. Then the solvent was removed, and the resultant residue was chromatographed over silica gel, eluting with petroleum ether to afford the desired product 6b (4.1 g, 85% yield, 97% HPLC purity):  $^1\text{H NMR}$  (400 MHz,  $\text{CDCl}_3$ ),  $\delta$  9.05 (s, 1H), 8.41 (s, 1H), 3.22 (s, 3H); MS (ESI, positive ion),  $m/z$  189.8 [ $\text{M} + \text{H}$ ] $^+$ .

**2-Chloro-*N*-cyclopropyl-5-nitropyrimidin-4-amine (6c):** yield, 4.1 g (75%, 97% HPLC purity);  $^1\text{H NMR}$  (400 MHz,  $\text{CDCl}_3$ ),  $\delta$  8.84 (s, 1H), 7.35 (s, 1H), 3.84 (m, 1H), 1.36 (m, 4H); MS (ESI, positive ion),  $m/z$  215.9 [ $\text{M} + \text{H}$ ] $^+$ .

**2-Chloro-*N*-isopropyl-5-nitropyrimidin-4-amine (6d):** yield, 3.3 g (90%, 97% HPLC purity);  $^1\text{H NMR}$  (400 MHz,  $\text{CDCl}_3$ ),  $\delta$  9.03 (s, 1H), 8.24 (s, 1H), 4.53 (m, 1H), 1.34 (d,  $J = 6.8$  Hz, 6H); MS (ESI, positive ion),  $m/z$  217.8 [ $\text{M} + \text{H}$ ] $^+$ .

**2-Chloro-*N*-cyclopentyl-5-nitropyrimidin-4-amine (6e):** yield, 4.6 g (75%, 97% HPLC purity);  $^1\text{H NMR}$  (400 MHz,  $\text{CDCl}_3$ ),  $\delta$  9.03 (s, 1H), 8.38 (s, 1H), 4.59 (m, 1H), 2.21–2.13 (m, 2H), 1.85–1.72 (m, 4H), 1.71–1.53 (m, 2H); MS (ESI, positive ion),  $m/z$  243.8 [ $\text{M} + \text{H}$ ] $^+$ .

**2-Chloro-*N*-cyclohexyl-5-nitropyrimidin-4-amine (6f):** yield, 3.6 g (76%, 97% HPLC purity);  $^1\text{H NMR}$  (400 MHz,  $\text{CDCl}_3$ ),  $\delta$  9.03 (s, 1H), 7.26 (s, 1H), 4.25–4.23 (m, 1H), 2.05–2.03 (m, 2H), 1.81–1.78 (m, 2H), 1.50–1.36 (m, 6H); MS (ESI, positive ion),  $m/z$  257.8 [ $\text{M} + \text{H}$ ] $^+$ .

**2-Chloro-5-nitro-*N*-phenylpyrimidin-4-amine (6g).** To a solution of 2,4-dichloro-5-nitropyrimidine (5 g, 25.7 mmol) in  $\text{CH}_2\text{Cl}_2$  (100 mL) was added *N,N*-diisopropylethylamine (4.3 mL, 25.7 mmol) and aniline (2.4 mL, 25.7 mmol) at 0 °C. The

reaction mixture was stirred for 5 h at room temperature, and then saturated salt water (200 mL) was added. The mixture was extracted with  $\text{CH}_2\text{Cl}_2$  (300 mL). The combined organic layer was dried over  $\text{MgSO}_4$  and concentrated to dryness. The residue was purified by recrystallization from diethyl ether: yield, 5.8 g (90%, 96% HPLC purity);  $^1\text{H NMR}$  (400 MHz,  $\text{DMSO-}d_6$ ),  $\delta$  10.45 (s, 1H), 9.10 (s, 1H), 7.54 (d,  $J = 8.0$  Hz, 2H), 7.45 (t,  $J = 7.6$  Hz, 2H), 7.29 (t,  $J = 7.6$  Hz, 1H); MS (ESI, positive ion),  $m/z$  251.9 [ $\text{M} + \text{H}$ ] $^+$ .

**2-Chloro-*N*-(3,5-dimethylphenyl)-5-nitropyrimidin-4-amine (6h).** The title compound was prepared from 5 and 3,5-dimethylaniline using the procedure previously described for compound 6f and was purified by recrystallization from diethyl ether: yield, 5.7 g (89%, 95% HPLC purity);  $^1\text{H NMR}$  (400 MHz,  $\text{DMSO-}d_6$ ),  $\delta$  10.32 (s, 1H), 9.14 (s, 1H), 7.31 (s, 2H), 6.94 (s, 1H), 2.30 (s, 6H); MS (ESI, positive ion),  $m/z$  279.9 [ $\text{M} + \text{H}$ ] $^+$ .

**General Procedure for the Synthesis of Compounds 7a–7h.** *N*<sup>2</sup>-(4-(4-Methylpiperazin-1-yl)phenyl)-5-nitropyrimidine-2,4-diamine (7a). A solution of 6a (3 g, 17.2 mmol) and 4 (3.3 g, 17.2 mmol) in *n*-butanol (200 mL) was stirred at 90 °C for 5 h. After this time, the reaction mixture was cooled to room temperature. The resulting precipitate was collected by filtration, rinsing with EtOH, to give compound 7a as its hydrochloride salt (4.3 g, 75% yield):  $^1\text{H NMR}$  (400 MHz,  $\text{CDCl}_3$ ),  $\delta$  9.07 (s, 1H), 8.52 (s, 2H), 8.40 (s, 1H), 7.55 (m, 2H), 7.10 (m, 2H), 3.31 (t,  $J = 4.8$  Hz, 4H), 2.81 (t,  $J = 4.8$  Hz, 4H), 2.30 (s, 3H); MS (ESI, positive ion),  $m/z$  330.5 [ $\text{M} + \text{H}$ ] $^+$ .

***N*<sup>4</sup>-Methyl-*N*<sup>2</sup>-(4-(4-methylpiperazin-1-yl)phenyl)-5-nitropyrimidine-2,4-diamine (7b):** yield, 2.6 g (75%, 95% HPLC purity);  $^1\text{H NMR}$  (400 MHz,  $\text{CDCl}_3$ ),  $\delta$  9.11 (s, 1H), 8.34 (s, 1H), 7.59 (s, 1H), 7.51 (m, 2H), 7.23 (m, 2H), 4.21 (s, 3H), 3.15 (t,  $J = 4.8$  Hz, 4H), 2.87 (t,  $J = 4.8$  Hz, 4H), 2.48 (s, 3H); MS (ESI, positive ion),  $m/z$  344.5 [ $\text{M} + \text{H}$ ] $^+$ .

***N*<sup>4</sup>-Cyclopropyl-*N*<sup>2</sup>-(4-(4-methylpiperazin-1-yl)phenyl)-5-nitropyrimidine-2,4-diamine (7c):** yield, 2.6 g (71%, 96% HPLC purity);  $^1\text{H NMR}$  (400 MHz,  $\text{CDCl}_3$ ),  $\delta$  9.08 (s, 1H), 8.39 (s, 1H), 7.90 (s, 1H), 7.58 (m, 2H), 6.94 (m, 2H), 4.32 (m, 1H), 3.05 (t,  $J = 4.8$  Hz, 4H), 2.90 (t,  $J = 4.8$  Hz, 4H), 2.67 (s, 3H), 1.39 (m, 4H); MS (ESI, positive ion),  $m/z$  370.6 [ $\text{M} + \text{H}$ ] $^+$ .

***N*<sup>4</sup>-Isopropyl-*N*<sup>2</sup>-(4-(4-methylpiperazin-1-yl)phenyl)-5-nitropyrimidine-2,4-diamine (7d):** yield, 2.8 g (73%, 95% HPLC purity);  $^1\text{H NMR}$  (400 MHz,  $\text{CDCl}_3$ ),  $\delta$  9.02 (s, 1H), 8.42 (s, 1H), 7.63 (s, 1H), 7.51 (m, 2H), 6.95 (m, 2H), 4.41 (m, 1H), 3.22 (t,  $J = 4.8$  Hz, 4H), 2.61 (t,  $J = 4.8$  Hz, 4H), 2.37 (s, 3H), 1.33 (d,  $J = 6.4$  Hz, 6H); MS (ESI, positive ion),  $m/z$  372.5 [ $\text{M} + \text{H}$ ] $^+$ .

***N*<sup>4</sup>-Cyclopentyl-*N*<sup>2</sup>-(4-(4-methylpiperazin-1-yl)phenyl)-5-nitropyrimidine-2,4-diamine (7e):** yield, 2.2 g (71%, 95% HPLC purity);  $^1\text{H NMR}$  (400 MHz,  $\text{CDCl}_3$ ),  $\delta$  9.03 (s, 1H), 8.47 (s, 1H), 7.69 (s, 1H), 7.51 (m, 2H), 7.11 (m, 2H), 4.43 (m, 1H), 3.28 (t,  $J = 4.8$  Hz, 4H), 2.67 (t,  $J = 4.8$  Hz, 4H), 2.45 (s, 3H), 2.23–2.15 (m, 2H), 1.86–1.74 (m, 4H), 1.72–1.50 (m, 2H); MS (ESI, positive ion),  $m/z$  398.6 [ $\text{M} + \text{H}$ ] $^+$ .

***N*<sup>4</sup>-Cyclohexyl-*N*<sup>2</sup>-(4-(4-methylpiperazin-1-yl)phenyl)-5-nitropyrimidine-2,4-diamine (7f):** yield, 2.6 g (67%, 95% HPLC purity);  $^1\text{H NMR}$  (400 MHz,  $\text{CDCl}_3$ ),  $\delta$  10.28 (s, 1H), 8.95 (s, 1H), 8.48 (s, 1H), 7.67 (d,  $J = 8.0$  Hz, 2H), 6.94 (d,  $J = 8.0$  Hz, 2H), 4.04 (m, 1H), 3.01 (s, 3H), 2.72 (s, 4H), 2.41 (s, 4H), 1.97 (s, 2H), 1.76–1.74 (m, 2H), 1.65–1.62 (m, 2H), 1.43–1.40 (m, 4H); MS (ESI, positive ion),  $m/z$  412.7 [ $\text{M} + \text{H}$ ] $^+$ .

*N*<sup>2</sup>-(4-(4-Methylpiperazin-1-yl)phenyl)-5-nitro-*N*<sup>4</sup>-phenylpyrimidine-2,4-diamine (**7g**): yield, 2.8 g (78%, 95% HPLC purity); <sup>1</sup>H NMR (400 MHz, DMSO-*d*<sub>6</sub>), δ 10.37 (s, 1H), 10.36 (s, 1H), 9.07 (s, 1H), 7.58 (d, *J* = 7.6 Hz, 2H), 7.43 (d, *J* = 7.6 Hz, 2H), 7.40 (m, 1H), 7.30–7.28 (m, 2H), 6.82 (d, *J* = 8.4 Hz, 2H), 3.30 (m, 4H), 2.79 (s, 3H), 2.49 (m, 4H); MS (ESI, positive ion), *m/z* 406.7 [M + H]<sup>+</sup>.

*N*<sup>4</sup>-(3,5-Dimethylphenyl)-*N*<sup>2</sup>-(4-(4-methylpiperazin-1-yl)phenyl)-5-nitropyrimidine-2,4-diamine (**7h**): yield, 2.1 g (76%, 95% HPLC purity); <sup>1</sup>H NMR (400 MHz, DMSO-*d*<sub>6</sub>), δ 10.37 (s, 1H), 10.33 (s, 1H), 9.07 (s, 1H), 7.50 (d, *J* = 8.8 Hz, 2H), 7.24 (s, 2H), 6.89 (s, 1H), 6.87 (d, *J* = 8.8 Hz, 2H), 3.76–3.73 (m, 2H), 3.50–3.48 (m, 2H), 3.16–3.14 (m, 2H), 3.01–2.97 (m, 2H), 2.82 (s, 3H), 2.26 (s, 6H); MS (ESI, positive ion), *m/z* 434.7 [M + H]<sup>+</sup>.

*N*<sup>2</sup>-(4-(4-Methylpiperazin-1-yl)phenyl)-*N*<sup>8</sup>-phenyl-9H-purine-2,8-diamine (**9a**). To a solution of the hydrochloride salt of **7a** (3 g, 8.2 mmol) in MeOH (60 mL) was added 10% Pd/C (300 mg), and the resulting suspension was stirred at 50 °C under an atmospheric pressure of H<sub>2</sub> for 6 h. Then the catalyst was filtered over dicalite. The filtrate was concentrated under high vacuum to afford the product **8a** as a black solid. This material was not purified but used directly in the next step.

A suspension of compound **8a** (1 g, 3.34 mmol), EDCI (0.8 g, 3.78 mmol), DIEA (0.6 mL, 3.78 mmol), and phenyl isothiocyanate (0.5 mL, 3.78 mmol) in CH<sub>2</sub>Cl<sub>2</sub> (20 mL) was refluxed for 12 h until TLC showed that the reaction was complete. The reaction mixture was evaporated under reduced pressure, and the residue was chromatographed over silica gel eluting with CH<sub>2</sub>Cl<sub>2</sub>/MeOH (20:1) to give a pale yellow solid, which was further washed with cold ethanol to afford pure product **9a** (0.64 g, 48% yield, 95% HPLC purity): <sup>1</sup>H NMR (400 MHz, DMSO-*d*<sub>6</sub>), δ 10.89 (s, 1H), 9.93 (s, 1H), 8.77 (s, 1H), 8.20 (s, 1H), 7.63 (d, *J* = 8.4 Hz, 2H), 7.34 (t, *J* = 6.8 Hz, 2H), 7.30 (d, *J* = 7.2 Hz, 2H), 7.00 (s, 1H), 6.87 (d, *J* = 8.8 Hz, 2H), 3.04 (t, *J* = 4.4 Hz, 4H), 2.46 (t, *J* = 4.4 Hz, 4H), 2.23 (s, 3H); MS (ESI, positive ion), *m/z* 401.9 [M + H]<sup>+</sup>.

9-Methyl-*N*<sup>2</sup>-(4-(4-methylpiperazin-1-yl)phenyl)-*N*<sup>8</sup>-phenyl-9H-purine-2,8-diamine (**9b**). An analogous reaction to that described for compound **9a**, but starting with **7b**, was used: yield, 0.7 g (40%, 95% HPLC purity); <sup>1</sup>H NMR (400 MHz, DMSO-*d*<sub>6</sub>), δ 9.11 (s, 1H), 9.02 (s, 1H), 8.32 (s, 1H), 7.88 (d, *J* = 8.0 Hz, 2H), 7.67 (d, *J* = 8.8 Hz, 2H), 7.33 (t, *J* = 8.0 Hz, 2H), 6.98 (t, *J* = 7.2 Hz, 1H), 6.87 (d, *J* = 8.0 Hz, 2H), 3.66 (s, 3H), 3.04 (m, 4H), 2.46 (m, 4H), 2.22 (s, 3H); MS (ESI, positive ion), *m/z* 415.7 [M + H]<sup>+</sup>.

9-Cyclopropyl-*N*<sup>2</sup>-(4-(4-methylpiperazin-1-yl)phenyl)-*N*<sup>8</sup>-phenyl-9H-purine-2,8-diamine (**9c**). An analogous reaction to that described for compound **9a**, but starting with **7c**, was used: yield, 0.9 g (41%, 97% HPLC purity); <sup>1</sup>H NMR (400 MHz, DMSO-*d*<sub>6</sub>), δ 9.00 (s, 1H), 8.87 (s, 1H), 8.31 (s, 1H), 7.89 (d, *J* = 8.0 Hz, 2H), 7.69 (d, *J* = 8.0 Hz, 2H), 7.34 (t, *J* = 8.0 Hz, 2H), 7.00 (t, *J* = 8.0 Hz, 1H), 6.88 (d, *J* = 8.0 Hz, 2H), 4.34 (m, 1H), 3.18–3.17 (br, 4H), 2.48–2.47 (br, 4H), 2.23 (s, 3H), 1.26–1.24 (m, 2H), 1.23–1.17 (m, 2H); MS (ESI, positive ion), *m/z* 441.7 [M + H]<sup>+</sup>.

9-Isopropyl-*N*<sup>2</sup>-(4-(4-methylpiperazin-1-yl)phenyl)-*N*<sup>8</sup>-phenyl-9H-purine-2,8-diamine (**9d**). An analogous reaction to that described for compound **9a**, but starting with **7d**, was used: yield, 0.6 g (37%, 96% HPLC purity); <sup>1</sup>H NMR (400 MHz, DMSO-*d*<sub>6</sub>), δ 9.09 (s, 1H), 9.07 (s, 1H), 8.36 (s, 1H), 7.83 (d, *J* = 8.0 Hz, 2H), 7.69 (d, *J* = 9.2 Hz, 2H), 7.33 (m, 2H), 6.97 (m, 3H), 4.92 (m, 1H), 3.44 (br, 4H), 3.17 (br, 4H), 2.81 (s, 3H),

1.67 (d, *J* = 6.8 Hz, 6H); MS (ESI, positive ion), *m/z* 443.8 [M + H]<sup>+</sup>.

9-Cyclopentyl-*N*<sup>2</sup>-(4-(4-methylpiperazin-1-yl)phenyl)-*N*<sup>8</sup>-phenyl-9H-purine-2,8-diamine (**9e**). An analogous reaction to that described for compound **9a**, but starting with **7e**, was used: yield, 0.6 g (48%, 95% HPLC purity); <sup>1</sup>H NMR (400 MHz, DMSO-*d*<sub>6</sub>), δ 8.99 (s, 1H), 8.97 (s, 1H), 8.35 (s, 1H), 7.81 (d, *J* = 8.0 Hz, 2H), 7.61 (d, *J* = 8.0 Hz, 2H), 7.33 (t, *J* = 8.0 Hz, 2H), 6.98 (t, *J* = 8.0 Hz, 1H), 6.87 (d, *J* = 8.0 Hz, 2H), 5.02–4.91 (m, 1H), 3.06–3.03 (m, 4H), 2.50–2.46 (m, 4H), 2.44 (s, 2H), 2.22 (s, 3H), 2.05 (s, 4H), 1.70 (s, 2H); MS (ESI, positive ion), *m/z* 469.9 [M + H]<sup>+</sup>.

9-Cyclohexyl-*N*<sup>2</sup>-(4-(4-methylpiperazin-1-yl)phenyl)-*N*<sup>8</sup>-phenyl-9H-purine-2,8-diamine (**9f**). An analogous reaction to that described for compound **9a**, but starting with **7f**, was used: yield, 0.28 g (35%, 96% HPLC purity); <sup>1</sup>H NMR (400 MHz, DMSO-*d*<sub>6</sub>), δ 9.04 (s, 1H), 8.99 (s, 1H), 8.34 (s, 1H), 7.80 (d, *J* = 8.0 Hz, 2H), 7.67 (d, *J* = 8.0 Hz, 2H), 7.33 (t, *J* = 8.0 Hz, 2H), 6.98 (t, *J* = 8.0 Hz, 1H), 6.87 (d, *J* = 8.0 Hz, 2H), 5.01–4.81 (m, 1H), 3.05 (s, 4H), 2.47 (s, 6H), 2.23 (s, 3H), 1.92–1.90 (m, 2H), 1.84–1.81 (m, 2H), 1.80–1.78 (m, 2H), 1.48–1.44 (m, 2H); MS (ESI, positive ion), *m/z* 483.7 [M + H]<sup>+</sup>.

*N*<sup>2</sup>-(4-(4-Methylpiperazin-1-yl)phenyl)-*N*<sup>8,9</sup>-diphenyl-9H-purine-2,8-diamine (**9g**). An analogous reaction to that described for compound **9a**, but starting with **7g**, was used: yield, 1.2 g (48%, 95% HPLC purity); <sup>1</sup>H NMR (400 MHz, DMSO-*d*<sub>6</sub>), δ 9.07 (s, 1H), 8.77 (s, 1H), 8.45 (s, 1H), 7.80 (d, *J* = 8.0 Hz, 2H), 7.67 (d, *J* = 8.0 Hz, 2H), 7.56–7.46 (m, 5H), 7.30 (t, *J* = 8.0 Hz, 2H), 6.98 (t, *J* = 8.0 Hz, 1H), 6.85 (s, 1H), 6.82 (s, 1H), 3.18 (s, 4H), 2.93 (s, 4H), 2.65 (s, 3H); MS (ESI, positive ion), *m/z* 477.7 [M + H]<sup>+</sup>.

9-(3,5-Dimethylphenyl)-*N*<sup>2</sup>-(4-(4-methylpiperazin-1-yl)phenyl)-*N*<sup>8</sup>-phenyl-9H-purine-2,8-diamine (**9h**). An analogous reaction to that described for compound **9a**, but starting with **7h**, was used: yield, 1.7 g (48%, 95% HPLC purity); <sup>1</sup>H NMR (400 MHz, DMSO-*d*<sub>6</sub>), δ 9.06 (s, 1H), 8.70 (s, 1H), 8.42 (s, 1H), 7.81 (d, *J* = 8.0 Hz, 2H), 7.60 (d, *J* = 8.0 Hz, 2H), 7.31 (t, *J* = 8.0 Hz, 2H), 7.21 (s, 3H), 6.82 (t, *J* = 8.0 Hz, 1H), 6.81 (d, *J* = 8.0 Hz, 2H), 3.12 (s, 4H), 2.78 (s, 4H), 2.45 (s, 3H), 2.40 (s, 6H); MS (ESI, positive ion), *m/z* 505.9 [M + H]<sup>+</sup>.

4-(4-Nitrophenyl)morpholine (**10a**). The title compound was prepared from **2** and morpholine using the procedure previously described for compound **3**: yield, 6.4 g (85%, 96% HPLC purity); <sup>1</sup>H NMR (400 MHz, DMSO-*d*<sub>6</sub>), δ 8.19 (d, *J* = 8.8 Hz, 2H), 7.58 (d, *J* = 8.8 Hz, 2H), 2.38 (br, 4H), 2.33 (br, 4H); MS (ESI, positive ion), *m/z* 209.5 [M + H]<sup>+</sup>.

4-Methyl-1-(4-nitrophenyl)piperidine (**10b**). The title compound was prepared from **2** and 4-methylpiperidine using the procedure previously described for compound **3**: yield, 5.4 g (70%, 96% HPLC purity); <sup>1</sup>H NMR (400 MHz, DMSO-*d*<sub>6</sub>), δ 8.02 (d, *J* = 8.0 Hz, 2H), 6.99 (d, *J* = 8.0 Hz, 2H), 4.02 (m, 2H), 2.96 (m, 2H), 1.72 (s, 1H), 1.66 (m, 2H), 1.12 (m, 2H), 0.91 (d, *J* = 4.0 Hz, 3H); MS (ESI, positive ion), *m/z* 221.5 [M + H]<sup>+</sup>.

2-(4-Nitrophenylamino)ethanol (**10c**). The title compound was prepared from **2** and ethanolamine using the procedure previously described for compound **3**: yield, 5.1 g (80%, 96% HPLC purity); <sup>1</sup>H NMR (400 MHz, DMSO-*d*<sub>6</sub>), δ 7.97 (d, *J* = 8.0 Hz, 2H), 7.29 (m, 1H), 6.65 (d, *J* = 8.0 Hz, 2H), 4.80 (m, 1H), 3.57 (m, 2H), 3.23 (m, 2H); MS (ESI, positive ion), *m/z* 183.3 [M + H]<sup>+</sup>.

*N*<sup>4</sup>-Cyclopentyl-*N*<sup>2</sup>-(4-morpholinophenyl)-5-nitropyrimidine-2,4-diamine (**12a**). A solution of compound **10a** (3 g,

14.4 mmol) in ethanol (250 mL) was purged with N<sub>2</sub>, and 10% Pd/C (0.3 g) was added. The mixture was placed under H<sub>2</sub> (1 atm) for 9 h. The mixture was purged with N<sub>2</sub> and filtered through a pad of Celite, rinsing with ethanol. The filtrate was concentrated to give compound **11a**. This compound was not purified but used directly in the next step.

A solution of **6e** (3 g, 12.4 mmol) and **11a** (2.2 g, 12.4 mmol) in *n*-butanol (200 mL) was stirred at 90 °C for 5 h. The reaction mixture was cooled to room temperature. The resulting precipitate was collected by filtration, rinsing with EtOH, to give compound **12a** as its hydrochloride salt (2.7 g, 51% yield): <sup>1</sup>H NMR (400 MHz, DMSO-*d*<sub>6</sub>), δ 10.29 (s, 1H), 8.94 (s, 1H), 8.52–8.50 (br, 1H), 7.69 (d, *J* = 8.0 Hz, 2H), 6.94 (d, *J* = 12.0 Hz, 2H), 4.45–4.44 (br, 1H), 3.73 (t, *J* = 6.0 Hz, 4H), 3.08 (t, *J* = 6.0 Hz, 4H), 2.06–2.04 (br, 2H), 1.73–1.71 (br, 2H), 1.62 (s, 4H); MS (ESI, positive ion), *m/z* 385.6 [M + H]<sup>+</sup>.

*N*<sup>4</sup>-Cyclopentyl-*N*<sup>2</sup>-(4-(4-methylpiperidin-1-yl)phenyl)-5-nitropyrimidine-2,4-diamine (**12b**). Compound **12b** was prepared following the procedure described for **12a**, substituting **10b** for **10a**: yield, 3.1 g (70%, 96% HPLC purity); <sup>1</sup>H NMR (400 MHz, DMSO-*d*<sub>6</sub>), δ 10.27 (s, 1H), 8.93 (s, 1H), 8.51 (br, 1H), 7.66 (d, *J* = 8.0 Hz, 2H), 6.93 (d, *J* = 8.0 Hz, 2H), 4.45 (s, 1H), 3.62 (br, 2H), 2.63 (br, 2H), 2.05 (m, 2H), 1.73–1.71 (m, 4H), 1.70–1.68 (m, 4H), 1.49 (br, 1H), 1.26–1.23 (m, 2H), 0.93 (d, *J* = 4.0 Hz, 3H); MS (ESI, positive ion), *m/z* 397.6 [M + H]<sup>+</sup>.

2-(4-(4-(Cyclopentylamino)-5-nitropyrimidin-2-ylamino)phenylamino)ethanol (**12c**). Compound **12c** was prepared following the procedure described for **12a**, substituting **10c** for **10a**: yield, 3.7 g (70%, 95% HPLC purity); <sup>1</sup>H NMR (400 MHz, DMSO-*d*<sub>6</sub>), δ 10.60 (s, 1H), 8.99 (s, 1H), 8.51 (s, 1H), 7.92 (s, 2H), 7.57 (d, *J* = 7.6 Hz, 2H), 5.04–4.71 (br, 3H), 4.48 (s, 2H), 3.72 (s, 2H), 2.06 (s, 2H), 1.66 (s, 2H), 1.64 (s, 4H); MS (ESI, positive ion), *m/z* 359.6 [M + H]<sup>+</sup>.

*N*<sup>4</sup>-Cyclopentyl-5-nitro-*N*<sup>2</sup>-phenylpyrimidine-2,4-diamine (**12d**). A solution of **6e** (3 g, 12.4 mmol) and aniline (1.2 g, 12.4 mmol) in *n*-butanol (200 mL) was stirred at 90 °C for 5 h. The reaction mixture was cooled to room temperature. The resulting precipitate was collected by filtration, rinsing with EtOH, to give compound **12d** (2.6 g, 70% yield, 95% HPLC purity): <sup>1</sup>H NMR (400 MHz, DMSO-*d*<sub>6</sub>), δ 10.43 (s, 1H), 8.99 (s, 1H), 8.50 (s, 1H), 7.80 (d, *J* = 8.0 Hz, 2H), 7.35 (t, *J* = 8.0 Hz, 2H), 7.08 (t, *J* = 8.0 Hz, 1H), 4.48 (s, 1H), 2.06–2.04 (m, 2H), 1.73–1.71 (m, 2H), 1.66–1.62 (m, 4H); MS (ESI, positive ion), *m/z* 300.5 [M + H]<sup>+</sup>.

*N*-(4-(4-(Cyclopentylamino)-5-nitropyrimidin-2-ylamino)phenyl)acetamide (**12e**). The title compound was prepared from **6e** and *N*-(4-aminophenyl)acetamide using the procedure previously described for compound **12d**: yield, 4.5 g (72%, 96% HPLC purity); <sup>1</sup>H NMR (400 MHz, DMSO-*d*<sub>6</sub>), δ 10.39 (s, 1H), 9.67 (s, 1H), 8.97 (s, 1H), 8.50 (s, 1H), 7.70 (d, *J* = 8.4 Hz, 2H), 7.55 (d, *J* = 8.4 Hz, 2H), 4.25 (s, 1H), 2.50 (s, 3H), 2.05 (s, 2H), 1.73 (s, 2H), 1.62 (s, 4H); MS (ESI, positive ion), *m/z* 357.4 [M + H]<sup>+</sup>.

9-Cyclopentyl-*N*<sup>2</sup>-(4-morpholinophenyl)-*N*<sup>8</sup>-phenyl-9H-purine-2,8-diamine (**14a**). To a solution of compound **12a** (3 g, 7.8 mmol) in MeOH (60 mL) was added 10% Pd/C (300 mg), and the resulting suspension was stirred at 50 °C under an atmospheric pressure of H<sub>2</sub> for 6 h. Then the catalyst was filtered over dicalite. The filtrate was concentrated under high vacuum to afford the product **13a** as a black solid. This material was not purified but used directly in the next step.

A suspension of compound **13a** (1 g, 2.82 mmol), EDCI (0.6 g, 3.11 mmol), DIEA (0.5 mL, 3.78 mmol), and phenyl isothiocyanate (0.4 mL, 3.78 mmol) in CH<sub>2</sub>Cl<sub>2</sub> (20 mL) was refluxed for 12 h until TLC showed that the reaction was complete. The reaction mixture was evaporated under reduced pressure, and the residue was chromatographed over silica gel eluting with CH<sub>2</sub>Cl<sub>2</sub>/MeOH (70:1) to give a white solid, which was further washed with diethyl ether to afford pure product **14a** (0.76 g, 60% yield, 95% HPLC purity): <sup>1</sup>H NMR (400 MHz, DMSO-*d*<sub>6</sub>), δ 9.00 (s, 1H), 8.99 (s, 1H), 8.34 (s, 1H), 7.81 (d, *J* = 8.0 Hz, 2H), 7.63 (d, *J* = 8.8 Hz, 2H), 7.33 (t, *J* = 8.0 Hz, 2H), 6.99–6.98 (m, 1H), 6.88 (d, *J* = 8.0 Hz, 2H), 4.97–4.93 (m, 1H), 3.74 (t, *J* = 4.0 Hz, 4H), 3.02 (t, *J* = 4.0 Hz, 4H), 2.47 (s, 2H), 2.05 (s, 4H), 1.70 (s, 2H); MS (ESI, positive ion), *m/z* 456.7 [M + H]<sup>+</sup>.

9-Cyclopentyl-*N*<sup>2</sup>-(4-(4-methylpiperidin-1-yl)phenyl)-*N*<sup>8</sup>-phenyl-9H-purine-2,8-diamine (**14b**). Compound **14b** was prepared following the procedure described for **14a**, substituting **12b** for **12a**: yield, 0.76 g (52%, 95% HPLC purity); <sup>1</sup>H NMR (400 MHz, DMSO-*d*<sub>6</sub>), δ 8.98 (s, 1H), 8.94 (s, 1H), 8.34 (s, 1H), 7.81 (d, *J* = 8.0 Hz, 2H), 7.59 (d, *J* = 8.0 Hz, 2H), 7.33 (t, *J* = 8.0 Hz, 2H), 6.98 (t, *J* = 8.0 Hz, 1H), 6.86 (d, *J* = 8.0 Hz, 2H), 5.02–4.91 (m, 1H), 2.50 (m, 1H), 2.04–1.99 (m, 4H), 1.71–1.68 (m, 4H), 0.94 (d, *J* = 4.0 Hz, 3H); MS (ESI, positive ion), *m/z* 468.9 [M + H]<sup>+</sup>.

2-(4-(9-Cyclopentyl-8-(phenylamino)-9H-purin-2-ylamino)phenylamino)ethanol (**14c**). Compound **14c** was prepared following the procedure described for **14a**, substituting **12c** for **12a**: yield, 0.66 g (56%, 95% HPLC purity); <sup>1</sup>H NMR (400 MHz, DMSO-*d*<sub>6</sub>), δ 9.46 (s, 1H), 9.05 (s, 1H), 8.69 (s, 1H), 7.88 (d, *J* = 8.0 Hz, 2H), 7.82 (d, *J* = 8.0 Hz, 2H), 7.30–7.23 (m, 5H), 7.10–7.07 (m, 1H), 7.01–6.98 (m, 1H), 4.95–4.91 (m, 1H), 4.16 (t, *J* = 7.2 Hz, 2H), 3.67 (t, *J* = 8.0 Hz, 2H), 2.51 (br, 2H), 2.06 (br, 4H), 1.71–1.70 (br, 2H); MS (ESI, positive ion), *m/z* 430.7 [M + H]<sup>+</sup>.

9-Cyclopentyl-*N*<sup>2</sup>,*N*<sup>8</sup>-diphenyl-9H-purine-2,8-diamine (**14d**). Compound **14d** was prepared following the procedure described for **14a**, substituting **12d** for **12a**: yield, 0.36 g (61%, 95% HPLC purity); <sup>1</sup>H NMR (400 MHz, DMSO-*d*<sub>6</sub>), δ 9.25 (s, 1H), 9.04 (s, 1H), 8.41 (s, 1H), 7.83 (d, *J* = 8.0 Hz, 2H), 7.78 (d, *J* = 8.0 Hz, 2H), 7.34 (t, *J* = 8.0 Hz, 2H), 7.26 (t, *J* = 8.0 Hz, 2H), 6.99 (t, *J* = 8.0 Hz, 1H), 6.89 (t, *J* = 8.0 Hz, 1H), 5.02–4.93 (m, 1H), 2.49 (s, 2H), 2.06 (s, 4H), 1.71 (s, 2H); MS (ESI, positive ion), *m/z* 371.6 [M + H]<sup>+</sup>.

*N*-(4-(9-Cyclopentyl-8-(phenylamino)-9H-purin-2-ylamino)phenyl)acetamide (**14e**). Compound **14e** was prepared following the procedure described for **14a**, substituting **12e** for **12a**: yield, 0.54 g (41%, 95% HPLC purity); <sup>1</sup>H NMR (400 MHz, DMSO-*d*<sub>6</sub>), δ 9.76 (s, 1H), 9.17 (s, 1H), 9.02 (s, 1H), 8.38 (s, 1H), 7.82 (d, *J* = 8.0 Hz, 2H), 7.67 (d, *J* = 8.9 Hz, 2H), 7.45 (d, *J* = 8.0 Hz, 2H), 7.33 (t, *J* = 8.0 Hz, 2H), 6.99 (t, *J* = 7.6 Hz, 1H), 4.99–4.93 (m, 1H), 2.50 (s, 4H), 2.04 (s, 3H), 1.99 (s, 2H), 1.71 (s, 2H); MS (ESI, positive ion), *m/z* 428.7 [M + H]<sup>+</sup>.

1-Nitryl-3-isothiocyanato-benzene (**17a**). To a solution of **15a** (1.5 g, 10.9 mmol) in EtOH (15 mL) were added CS<sub>2</sub> (1.9 mL, 32.7 mmol) and DABCO (7.36 g, 65.4 mmol). The reaction mixture was stirred at room temperature overnight. The resulting precipitate was collected by filtration, washed with ice-cold ethanol, and dried to yield **16a** as a pale yellow solid, which was used in the next step without further characterization and purification. Triphosgene (1.6 g, 5.5 mmol) was added slowly to a solution of **16a** in CH<sub>2</sub>Cl<sub>2</sub> at 0

°C. The reaction mixture was stirred at this temperature for an additional 1 h and then heated at 40 °C for 4 h; the reaction was quenched with water. The crude was extracted with CH<sub>2</sub>Cl<sub>2</sub> and then dried over MgSO<sub>4</sub>. Then the organic layer was concentrated, and the resultant residue was chromatographed over silica gel, eluting with petroleum ether to afford the desired product **17a** (1.1 g, 58% yield): MS (ESI, positive ion), *m/z* 181.41 [M + H]<sup>+</sup>.

**Compounds 17b–j were prepared from 15b–j in a manner identical to the preparation of 17a.** **1-Alkynyl-3-isothiocyanatobenzene (17b):** yield, 70%; MS (ESI, positive ion), *m/z* 160.10 [M + H]<sup>+</sup>.

**1-Methyl-3-isothiocyanatobenzene (17c):** yield, 61%; MS (ESI, positive ion), *m/z* 150.30 [M + H]<sup>+</sup>.

**1-Hydroxy-3-isothiocyanatobenzene (17d):** yield, 56%; MS (ESI, positive ion), *m/z* 152.3 [M + H]<sup>+</sup>.

**1-Chloro-3-isothiocyanatobenzene (17e):** yield, 58%; MS (ESI, positive ion), *m/z* 170.8 [M + H]<sup>+</sup>.

**1-Bromo-4-isothiocyanatobenzene (17f):** yield, 50%; MS (ESI, positive ion), *m/z* 215.3 [M + H]<sup>+</sup>.

**1-Fluoro-3-bromo-6-isothiocyanatobenzene (17g):** yield, 52%; MS (ESI, positive ion), *m/z* 233.1 [M + H]<sup>+</sup>.

**1,4-Dichloro-2-isothiocyanatobenzene (17h):** yield, 67%; MS (ESI, positive ion), *m/z* 205.1 [M + H]<sup>+</sup>.

**N-(4-Chlorophenyl)-3-isothiocyanatobenzamide (17i):** yield, 63%; MS (ESI, positive ion), *m/z* 289.9 [M + H]<sup>+</sup>.

**N-(3-Isothiocyanatophenyl)benzamide (17j):** yield, 60%; MS (ESI, positive ion), *m/z* 255.6 [M + H]<sup>+</sup>.

**Compounds 18a–j were prepared by condensation of 8e with various substituted phenyl isothiocyanates (17a–j) using the procedure previously described for compound 9e and were purified by column chromatography.** **9-Cyclopentyl-N<sup>2</sup>-(4-(4-methylpiperazin-1-yl)phenyl)-N<sup>8</sup>-(3-nitrophenyl)-9H-purine-2,8-diamine (18a):** yield, 1.1 g (46%, 95% HPLC purity); <sup>1</sup>H NMR (400 MHz, DMSO-*d*<sub>6</sub>), δ 9.54 (s, 1H), 9.05 (s, 1H), 8.82 (s, 1H), 8.45 (s, 1H), 8.32 (d, *J* = 7.6 Hz, 1H), 7.83 (d, *J* = 8.0 Hz, 1H), 7.63 (s, 1H), 7.61 (d, *J* = 8.0 Hz, 2H), 6.95 (d, *J* = 8.8 Hz, 2H), 4.98–4.94 (m, 1H), 3.05 (s, 4H), 2.48 (s, 2H), 2.48 (s, 4H), 2.23 (s, 3H), 2.06 (s, 4H), 1.71 (s, 2H); MS (ESI, positive ion), *m/z* 514.7 [M + H]<sup>+</sup>.

**9-Cyclopentyl-N<sup>8</sup>-(3-ethynylphenyl)-N<sup>2</sup>-(4-(4-methylpiperazin-1-yl)phenyl)-9H-purine-2,8-diamine (18b):** yield, 1.3 g (41%, 95% HPLC purity); <sup>1</sup>H NMR (400 MHz, DMSO-*d*<sub>6</sub>), δ 9.26 (s, 1H), 9.13 (s, 1H), 8.43 (s, 1H), 8.09 (s, 1H), 7.85 (d, *J* = 8.0 Hz, 1H), 7.68 (d, *J* = 8.0 Hz, 2H), 7.35 (t, *J* = 8.0 Hz, 1H), 7.09 (d, *J* = 8.0 Hz, 1H), 6.95 (d, *J* = 8.0 Hz, 2H), 5.02–4.98 (m, 1H), 4.20 (s, 1H), 3.70 (br, 2H), 3.47 (br, 2H), 3.18 (br, 2H), 3.00 (br, 2H), 2.83 (s, 3H), 2.46 (br, 2H), 2.05 (br, 4H), 1.71 (br, 2H); MS (ESI, positive ion), *m/z* 493.9 [M + H]<sup>+</sup>.

**9-Cyclopentyl-N<sup>2</sup>-(4-(4-methylpiperazin-1-yl)phenyl)-N<sup>8</sup>-*m*-tolyl-9H-purine-2,8-diamine (18c):** yield, 1.3 g (42%, 95% HPLC purity); <sup>1</sup>H NMR (400 MHz, DMSO-*d*<sub>6</sub>), δ 9.08 (s, 1H), 9.02 (s, 1H), 8.37 (s, 1H), 7.68–7.62 (m, 4H), 7.22 (m, 1H), 6.93 (d, *J* = 8.8 Hz, 2H), 6.80 (d, *J* = 7.6 Hz, 1H), 4.99 (m, 1H), 3.67 (m, 2H), 3.44 (m, 2H), 3.03 (m, 4H), 2.81 (s, 3H), 2.45 (m, 2H), 2.31 (s, 3H), 2.04 (m, 4H), 1.69 (m, 2H); MS (ESI, positive ion), *m/z* 483.9 [M + H]<sup>+</sup>.

**3-(9-Cyclopentyl-2-(4-(4-methylpiperazin-1-yl)phenylamino)-9H-purin-8-ylamino)phenol (18d):** yield, 0.5 g (36%, 95% HPLC purity); <sup>1</sup>H NMR (400 MHz, DMSO-*d*<sub>6</sub>), δ 9.36 (s, 1H), 9.07 (s, 1H), 8.93 (s, 1H), 8.35 (s, 1H), 7.67 (d, *J*

= 9.2 Hz, 2H), 7.38 (s, 1H), 7.16 (d, *J* = 9.2 Hz, 1H), 7.10–7.08 (m, 1H), 6.93 (d, *J* = 9.2 Hz, 2H), 6.39 (s, 1H), 4.98–4.96 (m, 1H), 3.43 (m, 2H), 3.34 (m, 2H), 3.16 (m, 4H), 2.80 (s, 3H), 2.46 (m, 2H), 2.04 (m, 4H), 1.69 (m, 2H); MS (ESI, positive ion), *m/z* 485.9 [M + H]<sup>+</sup>.

**N<sup>8</sup>-(3-Chlorophenyl)-9-cyclopentyl-N<sup>2</sup>-(4-(4-methylpiperazin-1-yl)phenyl)-9H-purine-2,8-diamine (18e):** yield, 0.7 g (45%, 95% HPLC purity); <sup>1</sup>H NMR (400 MHz, DMSO-*d*<sub>6</sub>), δ 9.38 (s, 1H), 9.13 (s, 1H), 8.44 (s, 1H), 8.11 (s, 1H), 7.75 (d, *J* = 8.0 Hz, 1H), 7.65 (d, *J* = 8.4 Hz, 2H), 7.35 (m, 1H), 7.02 (m, 1H), 6.94 (d, *J* = 8.8 Hz, 2H), 5.01 (m, 1H), 3.43 (m, 4H), 3.10 (m, 4H), 2.82 (s, 3H), 2.45 (m, 2H), 2.05 (m, 4H), 1.70 (m, 2H); MS (ESI, positive ion), *m/z* 505.1 [M + H]<sup>+</sup>.

**N<sup>8</sup>-(4-Bromophenyl)-9-cyclopentyl-N<sup>2</sup>-(4-(4-methylpiperazin-1-yl)phenyl)-9H-purine-2,8-diamine (18f):** yield, 0.7 g (48%, 95% HPLC purity); <sup>1</sup>H NMR (400 MHz, DMSO-*d*<sub>6</sub>), δ 9.22 (s, 1H), 9.09 (s, 1H), 8.39 (s, 1H), 7.83 (d, *J* = 9.2 Hz, 2H), 7.66 (d, *J* = 8.0 Hz, 2H), 7.51 (d, *J* = 8.0 Hz, 2H), 6.93 (d, *J* = 8.0 Hz, 2H), 4.98–4.94 (m, 1H), 3.15 (m, 4H), 2.75 (m, 4H), 2.46 (s, 3H), 2.05 (m, 4H), 1.68 (m, 2H), 1.23 (m, 2H); MS (ESI, positive ion), *m/z* 548.6 [M + H]<sup>+</sup>.

**N<sup>8</sup>-(4-Bromo-2-fluorophenyl)-9-cyclopentyl-N<sup>2</sup>-(4-(4-methylpiperazin-1-yl)phenyl)-9H-purine-2,8-diamine (18g):** yield, 0.6 g (46%, 95% HPLC purity); <sup>1</sup>H NMR (400 MHz, DMSO-*d*<sub>6</sub>), δ 9.06 (s, 1H), 8.93 (s, 1H), 8.35 (s, 1H), 7.88–7.83 (m, 1H), 7.62 (d, *J* = 8.0 Hz, 2H), 7.59 (s, 1H), 7.40 (d, *J* = 8.0 Hz, 1H), 6.88 (d, *J* = 8.0 Hz, 2H), 4.90–4.86 (m, 1H), 3.10 (m, 4H), 2.62 (m, 4H), 2.43 (m, 2H), 2.34 (s, 3H), 2.03 (m, 4H), 1.68 (m, 2H); MS (ESI, positive ion), *m/z* 566.7 [M + H]<sup>+</sup>.

**9-Cyclopentyl-N<sup>8</sup>-(2,5-dichlorophenyl)-N<sup>2</sup>-(4-(4-methylpiperazin-1-yl)phenyl)-9H-purine-2,8-diamine (18h):** yield, 0.9 g (47%, 95% HPLC purity); <sup>1</sup>H NMR (400 MHz, DMSO-*d*<sub>6</sub>), δ 9.02 (s, 1H), 8.62 (s, 1H), 8.37 (s, 1H), 7.91 (s, 1H), 7.59 (d, *J* = 8.4 Hz, 2H), 7.49 (d, *J* = 7.6 Hz, 1H), 7.10 (m, 1H), 6.86 (d, *J* = 9.2 Hz, 2H), 4.91 (m, 1H), 3.04 (m, 4H), 2.45 (m, 4H), 2.31 (m, 2H), 2.22 (s, 3H), 2.00 (m, 4H), 1.67 (m, 2H); MS (ESI, positive ion), *m/z* 623.5 [M + H]<sup>+</sup>.

**N-(4-Chlorophenyl)-3-(9-cyclopentyl-2-(4-(4-methylpiperazin-1-yl)phenylamino)-9H-purin-8-ylamino)benzamide (18i):** yield, 0.8 g (49%, 95% HPLC purity); <sup>1</sup>H NMR (400 MHz, DMSO-*d*<sub>6</sub>), δ 10.42 (s, 1H), 9.36 (s, 1H), 9.12 (s, 1H), 8.41 (s, 1H), 8.26 (s, 1H), 8.19 (d, *J* = 8.0 Hz, 1H), 7.84 (d, *J* = 9.2 Hz, 2H), 7.67 (d, *J* = 8.8 Hz, 2H), 7.57 (d, *J* = 7.6 Hz, 1H), 7.49 (d, *J* = 7.8 Hz, 1H), 7.42 (d, *J* = 8.8 Hz, 2H), 6.94 (d, *J* = 8.8 Hz, 2H), 4.99 (m, 1H), 3.85–3.45 (br, 2H), 3.20–2.90 (br, 4H), 2.80 (s, 3H), 2.46–2.39 (br, 4H), 2.05 (m, 4H), 1.71 (m, 2H); MS (ESI, positive ion), *m/z* 623.2 [M + H]<sup>+</sup>.

**N-(3-(9-Cyclopentyl-2-(4-(4-methylpiperazin-1-yl)phenylamino)-9H-purin-8-ylamino)phenyl)benzamide (18j):** yield, 0.8 g (49%, 95% HPLC purity); <sup>1</sup>H NMR (400 MHz, DMSO-*d*<sub>6</sub>), δ 10.30 (s, 1H), 9.15 (s, 1H), 9.05 (s, 1H), 8.36 (s, 1H), 8.26 (s, 1H), 7.98 (d, *J* = 7.2 Hz, 2H), 7.67 (s, 1H), 7.64 (d, *J* = 8.8 Hz, 2H), 7.59 (d, *J* = 6.8 Hz, 1H), 7.55 (d, *J* = 6.8 Hz, 2H), 7.52 (s, 1H), 7.30 (d, *J* = 6.8 Hz, 1H), 6.90 (d, *J* = 8.8 Hz, 2H), 5.00 (m, 1H), 3.17–3.05 (br, 4H), 2.82 (s, 3H), 2.50–2.40 (br, 4H), 2.47 (m, 2H), 2.05 (m, 4H), 1.71–1.70 (br, 2H); MS (ESI, positive ion), *m/z* 588.9 [M + H]<sup>+</sup>.

**Kinase Inhibition and Binding Affinity Assays.** Kinase inhibition profiles were obtained using KinaseProfiler services provided by Millipore, and ATP concentrations used are the ATP *K<sub>m</sub>* of corresponding kinases. Binding affinities were

measured through KINOMEscan services provided by DiscoverRx (no ATP used according to the protocol).

**Cell Lines and Cell Culture Conditions.** Cell lines were acquired from the American Type Culture Collection (Manassas, VA, USA) except those specifically mentioned. All cell lines were cultured in the designated medium containing 10% FBS (v/v) at 37 °C in a humidified 5% CO<sub>2</sub> incubator and passaged for <6 months after receipt or resuscitation.

**Cell Viability Assays.** The viability of cells was determined using the MTT assay method. The cell lines were seeded (2000–20000 cells per well, depending on the cell type) in 96-well plates. After incubation for 24 h in serum-containing media, the cells were treated with inhibitors (0–10 μg/mL) diluted with culture medium for 72 h at 37 °C under a 5% CO<sub>2</sub> atmosphere. Thereafter, 20 μL of the MTT reagent (5 mg/mL) was added to each well, and the plates were incubated for 2–4 h at 37 °C. For the adherent cells, the media and MTT were carefully aspirated from each well, and the formazan crystals were dissolved in 150 μL of DMSO. For the suspended cells, 50 μL of 20% acidified SDS (w/v) was added to each well, and the cells were incubated overnight. Finally, the absorbance at 570 nm was read using a Multiskan MK3 ELISA photometer (Thermo Scientific). All experiments were performed in triplicate.

**Western Blot Assays.** The HCC827 immunoblot studied cells treated with either compound **9e** or gefitinib (0–1 μmol/L) for 8 h. Whole-cell protein lysates were prepared and centrifuged for 15 min at 13000 rpm and 4 °C to remove any insoluble material. The total proteins were determined using the Bradford method, and an equivalent quantity of protein was combined with an SDS-PAGE loading buffer (Beyotime) according to the manufacturer's instructions. Proteins were separated via gel electrophoresis on 5–10% polyacrylamide gels and transferred to polyvinylidene fluoride membranes (Millipore). Antibody–antigen complexes were detected using an enhanced chemiluminescence system (Millipore). The following antibodies from Cell Signaling Technology were used at a 1:1000 dilution: anti-EGFR, anti-pEGFR<sup>Tyr1068</sup>, anti-AKT, anti-pAKT<sup>Ser473</sup>, anti-ERK, and anti-pERK<sup>Thr202/Tyr204</sup>. The anti-β-actin primary antibody was used at a 1:2000 dilution, and the horseradish peroxidase-coupled secondary antibodies were used at a 1:5000 dilution. For the H1975 Western blot assay, cells were incubated overnight in serum-free media. Compound **9e** and gefitinib (0–10 μmol/L) were then added. After 3 h, the cells were stimulated with 100 ng/mL human recombinant EGF (Sigma) for 15 min. Western blots were performed on whole-cell extracts as described above.

**Immunohistochemistry.** Tumor-bearing female BALB/c mice were given compound **9e** (1 or 50 mg/kg) and a vehicle once daily via oral gavage, and the tumors were harvested 3 or 10 days later. The tumors were fixed with formalin and embedded in paraffin. For immunohistochemistry staining, antigen retrieval was performed on paraffin-embedded tumor sections and the following primary antibodies were used: phospho-EGFR (Cell Signaling Technology, 1:100) and Ki67 (Thermo Fisher Scientific, 1:100). A polymer detection system (Dako EnVision+ K4007) was used for secondary detection, and the sections were counterstained with Carazzi's hematoxylin. Images were captured using an Olympus digital camera attached to a light microscope.

**Pharmacokinetic Assessments.** Catheters were surgically placed into the femoral veins of male Sprague–Dawley rats (HFK Biotechnology, Beijing, China) to collect serial blood

samples. The animals were fasted overnight prior to dosing, and food was withheld until 4 h after dosing. Compound **9e** was formulated for oral administration in 5% DMSO/15% PEG/80% sterile water at a target concentration of 4 mg/mL. The mice (220–250 g) were administered a single dose of 20 mg/kg compound **9e** via oral gavage. Blood was collected in heparin-containing tubes, and the plasma was isolated by centrifugation. The plasma concentrations of compound **9e** were determined using liquid–liquid extraction followed by high-performance liquid chromatography (HPLC) with tandem mass spectrometric detection (3200 QTRAP system; Applied Biosystems). Noncompartmental pharmacokinetic parameters were obtained from the plasma concentration–time profiles using DAS software (Enterprise version 2.0; Mathematical Pharmacology Professional Committee of China).

**Xenograft Models.** All animal experiments were approved by the Animal Care and Use Committee of Sichuan University. Cells were harvested during the exponential growth phase, washed three times with serum-free medium, and resuspended at a concentration of  $5 \times 10^7$ – $1 \times 10^8$  cells/mL. Tumor xenograft models were established by subcutaneously injecting 100 μL of tumor cell suspension into the right flank of female BALB/c nude mice (6–8 weeks old). The mice were randomized into four or five groups (six mice per group) prior to treatment with compound **9e**, gefitinib, or BIBW2992. The animals were given compound **9e** (1–50 mg/kg), gefitinib (100 mg/kg), BIBW2992 (20 mg/kg), or vehicle alone (25% PEG400 plus 5% DMSO in sterile water) once daily via oral gavage. Tumors were measured twice weekly using calipers, and their volume was calculated using the following formula: tumor volume =  $a \times b^2 \times 0.52$  ( $a$  = long diameter;  $b$  = short diameter).

**Molecular Docking Study.** All molecular docking studies were carried out on GOLD (Genetic Optimization of Ligand Docking) 4.0.<sup>31</sup> GOLD uses a genetic algorithm to dock flexible ligands into protein binding sites. The crystal structure (PDB entry 2JIU) of the kinase domain of EGFR (T790M) bound to the inhibitor compound AEE788 was used in the docking studies.<sup>32</sup> Hydrogen atoms were added to the protein using Accelrys Discovery Studio 2.55. The Charmm force field was assigned. The binding site was defined as a sphere containing the residues that remain within 10 Å of the ligand, an area large enough to cover the ATP-binding region at the active site.

In the process of hit discovery, molecular docking (GOLD) was performed against an in-house focused virtual library containing approximately 650 000 known kinase inhibitors and kinase inhibitor-like compounds; these compounds were selected in advance from several chemical libraries including BindingDB, ChemBl, Specs, and Enamine, as well as a database of chemicals synthesized by us. This focused virtual library contains all of the kinase inhibitors presented in BindingDB and ChemBl. The 3D conformations of compounds in virtual screening were generated by GOLD. The ID-Score scoring function proposed by us was calculated for ranking the screening compounds.

## ■ AUTHOR INFORMATION

### Corresponding Author

\*Phone: +86-28-85164063. Fax: +86-28-85164060. E-mail: yangsy@scu.edu.cn;

### Author Contributions

#These authors contributed equally to this work.

## Notes

The authors declare no competing financial interest.

## ACKNOWLEDGMENTS

This work was supported by the National Natural Science Foundation of China (81172987), the 973 Program (2013CB967204), the National S&T Major Project (2012ZX09102-101-002), and the 863 Hi-Tech Program (2012AA020301, 2012AA020308).

## ABBREVIATIONS USED

NSCLC, non-small-cell lung cancer; EGFR, epidermal growth factor receptor; SAR, structure-activity relationship; DABCO, 1,4-diaza[2.2.2]bicyclooctane; EDCI, 1-(3-dimethylaminopropyl)-3-ethylcarbodiimide hydrochloride; ERK, extracellular signal-regulated kinase; TLC, thin layer chromatography; DIEA, *N,N*-diisopropylethylamine

## REFERENCES

- (1) Siegel, R.; Naishadham, D.; Jemal, A. Cancer statistics. *CA Cancer J. Clin.* **2012**, *62*, 10–29.
- (2) Sequist, L. V.; Martins, R. G.; Spigel, D.; Grunberg, S. M.; Spira, A.; Jänne, P. A.; Joshi, V. A.; McCollum, D.; Evans, T. L.; Muzikansky, A.; Kuhlmann, G. L.; Han, M.; Goldberg, J. S.; Settleman, J.; Iafrate, A. J.; Engelman, J. A.; Haber, D. A.; Johnson, B. E.; Lynch, T. J. First-line gefitinib in patients with advanced non-small-cell lung cancer harboring somatic EGFR mutations. *J. Clin. Oncol.* **2008**, *26*, 2442–2449.
- (3) Sharma, S. V.; Bell, D. W.; Settleman, J.; Haber, D. A. Epidermal growth factor receptor mutations in lung cancer. *Nat. Rev. Cancer.* **2007**, *7*, 169–181.
- (4) Johnson, J. R.; Cohen, M.; Sridhara, R.; Chen, Y. F.; Williams, G. M.; Duan, J.; Gobburu, J.; Booth, B.; Benson, K.; Leighton, J.; Hsieh, L. S.; Chidambaram, N.; Zimmerman, P.; Pazdur, R. Approval summary for erlotinib for treatment of patients with locally advanced or metastatic non-small cell lung cancer after failure of at least one prior chemotherapy regimen. *Clin. Cancer Res.* **2005**, *11*, 6414–6421.
- (5) Han, S. W.; Kim, T. Y.; Hwang, P. G.; Jeong, S.; Kim, J.; Choi, I. S.; Oh, D. Y.; Kim, J. H.; Kim, D. W.; Chung, D. H.; Im, S. A.; Kim, Y. T.; Lee, J. S.; Heo, D. S.; Bang, Y. J.; Kim, N. K. Predictive and prognostic impact of epidermal growth factor receptor mutation in non-small-cell lung cancer patients treated with gefitinib. *J. Clin. Oncol.* **2005**, *23*, 2493–2501.
- (6) Greulich, H.; Chen, T. H.; Feng, W.; Jänne, P. A.; Alvarez, J. V.; Zappaterra, M.; Bulmer, S. E.; Frank, D. A.; Hahn, W. C.; Sellers, W. R.; Meyerson, M. Oncogenic transformation by inhibitor-sensitive and -resistant EGFR mutants. *PLoS Med.* **2005**, *2*, e313.
- (7) Ciardiello, F.; Tortora, G. EGFR antagonists in cancer treatment. *N. Engl. J. Med.* **2008**, *358*, 1160–1174.
- (8) Sordella, R.; Bell, D. W.; Haber, D. A.; Settleman, J. Gefitinib-sensitizing EGFR mutations in lung cancer activate antiapoptotic pathways. *Science* **2004**, *305*, 1163–1167.
- (9) Mok, T. S.; Wu, Y. L.; Thongprasert, S.; Yang, C. H.; Chu, D. T.; Saijo, N.; Sunpaweravong, P.; Han, B.; Margono, B.; Ichinose, Y.; Nishiwaki, Y.; Ohe, Y.; Yang, J. J.; Chewaskulyong, B.; Jiang, H.; Duffield, E. L.; Watkins, C. L.; Armour, A. A.; Fukuoka, M. Gefitinib or carboplatin-paclitaxel in pulmonary adenocarcinoma. *N. Engl. J. Med.* **2009**, *361*, 947–957.
- (10) Kobayashi, S.; Boggon, T. J.; Dayaram, T.; Jänne, P. A.; Kocher, O.; Meyerson, M.; Johnson, B. E.; Eck, M. J.; Tenen, D. G.; Halmos, B. EGFR mutation and resistance of non-small-cell lung cancer to gefitinib. *N. Engl. J. Med.* **2005**, *352*, 786–792.
- (11) Pao, W.; Miller, V. A.; Politi, K. A.; Riely, G. J.; Somwar, R.; Zakowski, M. F.; Kris, M. G.; Varmus, H. Acquired resistance of lung adenocarcinomas to gefitinib or erlotinib is associated with a second mutation in the EGFR kinase domain. *PLoS Med.* **2005**, *2*, e73.
- (12) Kwak, E. L.; Sordella, R.; Bell, D. W.; Godin-Heymann, N.; Okimoto, R. A.; Brannigan, B. W.; Harris, P. L.; Driscoll, D. R.; Fidias, P.; Lynch, T. J.; Rabindran, S. K.; McGinnis, J. P.; Wissner, A.; Sharma, S. V.; Isselbacher, K. J.; Settleman, J.; Haber, D. A. Irreversible inhibitors of the EGF receptor may circumvent acquired resistance to gefitinib. *Proc. Natl. Acad. Sci. U.S.A.* **2005**, *102*, 7665–7670.
- (13) Yun, C. H.; Mengwasser, K. E.; Toms, A. V.; Woo, M. S.; Greulich, H.; Wong, K. K.; Meyerson, M.; Eck, M. J. The T790M mutation in EGFR kinase causes drug resistance by increasing the affinity for ATP. *Proc. Natl. Acad. Sci. U.S.A.* **2008**, *105*, 2070–2075.
- (14) Eck, M. J.; Yun, C. H. Structural and mechanistic underpinnings of the differential drug sensitivity of EGFR mutations in non-small cell lung cancer. *Biochim. Biophys. Acta* **2010**, *1804*, 559–566.
- (15) Mishani, E.; Abourbeh, G.; Jacobson, O.; Dissoki, S.; Ben Daniel, R.; Rozen, Y.; Shaul, M.; Levitzki, A. High-affinity epidermal growth factor receptor (EGFR) irreversible inhibitors with diminished chemical reactivities as positron emission tomography (PET)-imaging agent candidates of EGFR overexpressing tumors. *J. Med. Chem.* **2005**, *48*, 5337–5348.
- (16) Chang, S.; Zhang, L.; Xu, S.; Luo, J.; Lu, X.; Zhang, Z.; Xu, T.; Liu, Y.; Tu, Z.; Xu, Y.; Ren, X.; Geng, M.; Ding, J.; Pei, D.; Ding, K. Design, synthesis, and biological evaluation of novel conformationally constrained inhibitors targeting epidermal growth factor receptor threonine<sup>790</sup> → methionine<sup>790</sup> mutant. *J. Med. Chem.* **2012**, *55*, 2711–2723.
- (17) Zhou, W. J.; Ercan, D.; Chen, L.; Yun, C. H.; Li, D.; Capelletti, M.; Cortot, A. B.; Chirieac, L.; Iacob, R. E.; Padera, R.; Engen, J. R.; Wong, K. K.; Eck, M. J.; Gray, N. S.; Jänne, P. A. Novel mutant-selective EGFR kinase inhibitors against EGFR T790M. *Nature* **2009**, *462*, 1070–1074.
- (18) Kwak, E. L.; Sordella, R.; Bell, D. W.; Godin, H. N.; Okimoto, R. A.; Brannigan, B. W.; Harris, P. L.; Driscoll, D. R.; Fidias, P.; Lynch, T. J.; Rabindran, S. K.; McGinnis, J. P.; Wissner, A.; Sharma, S. V.; Isselbacher, K. J.; Settleman, J.; Haber, D. A. Irreversible inhibitors of the EGF receptor may circumvent acquired resistance to gefitinib. *Proc. Natl. Acad. Sci. U.S.A.* **2005**, *102*, 7665–7670.
- (19) Belani, C. P. The role of irreversible EGFR inhibitors in the treatment of non-small cell lung cancer: overcoming resistance to reversible EGFR inhibitors. *Cancer Invest.* **2010**, *28*, 413–423.
- (20) Wong, K. K. HKI-272 in non small cell lung cancer. *Clin. Cancer Res.* **2007**, *13*, 4593–4596.
- (21) Erlichman, C.; Hidalgo, M.; Boni, J. P.; Martins, P.; Quinn, S. E.; Zacharchuk, C.; Amorusi, P.; Adjei, A. A.; Rowinsky, E. K. Phase I study of EKB-569, an irreversible inhibitor of the epidermal growth factor receptor, in patients with advanced solid tumors. *J. Clin. Oncol.* **2006**, *24*, 2252–2260.
- (22) Li, D.; Ambrogio, L.; Shimamura, T.; Kubo, S.; Takahashi, M.; Chirieac, L. R.; Padera, R. F.; Shapiro, G. I.; Baum, A.; Himmelsbach, F.; Rettig, W. J.; Meyerson, M.; Solca, F.; Greulich, H.; Wong, K. K. BIBW2992, an irreversible EGFR/HER2 inhibitor highly effective in preclinical lung cancer models. *Oncogene* **2008**, *27*, 4702–4711.
- (23) Engelman, J. A.; Zejnullahu, F.; Gale, C. M.; Lifshits, E.; Gonzales, A. J.; Shimamura, T.; Zhao, F.; Vincent, P. W.; Naumov, G. N.; Bradner, J. E.; Althaus, I. W.; Gandhi, L.; Shapiro, G. I.; Nelson, J. M.; Heymach, J. V.; Meyerson, M.; Wong, K. K.; Jänne, P. A. PF00299804, an irreversible Pan-ERBB inhibitor, is effective in lung cancer models with EGFR and ERBB2 mutations that are resistant to gefitinib. *Cancer Res.* **2007**, *67*, 11924–11932.
- (24) Sos, M. L.; Rode, H. B.; Heynck, S.; Peifer, M.; Fischer, F.; Klüter, S.; Pawar, V. G.; Reuter, C.; Heuckmann, J. M.; Weiss, J.; Rüdigerkeit, L.; Rabiller, M.; Koker, M.; Simard, J. R.; Getlik, M.; Yuza, Y.; Chen, T. H.; Greulich, H.; Thomas, R. K.; Rauh, D. Chemogenomic profiling provides insights into the limited activity of irreversible EGFR inhibitors in tumor cells expressing the T790M EGFR resistance mutation. *Cancer Res.* **2010**, *70*, 868–874.
- (25) Kim, Y.; Ko, J.; Cui, Z.; Abolhoda, A.; Ahn, J. S.; Ou, S. H.; Ahn, M. J.; Park, K. The EGFR T790M mutation in acquired resistance to an irreversible second-generation EGFR inhibitor. *Mol. Cancer Ther.* **2012**, *11*, 784–791.

(26) Ercan, D.; Zejnullahu, K.; Yonesaka, K.; Xiao, Y.; Capelletti, M.; Rogers, A.; Lifshits, E.; Brown, A.; Lee, C.; Christensen, J. G.; Kwiatkowski, D. J.; Engelman, J. A.; Jänne, P. A. Amplification of EGFR T790M causes resistance to an irreversible EGFR inhibitor. *Oncogene* **2010**, *29*, 2346–2356.

(27) Pan, Y.; Xu, Y.; Feng, S.; Luo, S.; Zheng, R.; Yang, J.; Wang, L.; Zhong, L.; Yang, H. Y.; Wang, B. L.; Yu, Y.; Liu, J.; Cao, Z.; Wang, X.; Ji, P.; Wang, Z.; Chen, X.; Zhang, S.; Wei, Y. Q.; Yang, S. Y. SKLB1206, a novel orally available multikinase inhibitor targeting EGFR activating and T790M mutants, ErbB2, ErbB4, and VEGFR2, displays potent antitumor activity both in vitro and in vivo. *Mol. Cancer Ther.* **2012**, *11*, 952–962.

(28) Antonello, A.; Tarozzi, A.; Morroni, F.; Cavalli, A.; Rosini, M.; Hrelia, P.; Bolognesi, M. L.; Melchiorre, C. Multitarget-directed drug design strategy: a novel molecule designed to block epidermal growth factor receptor (EGFR) and to exert proapoptotic effects. *J. Med. Chem.* **2006**, *49*, 6642–6645.

(29) Wu, C. H.; Coumar, M. S.; Chu, C. Y.; Lin, W. H.; Chen, Y. R.; Chen, C. T.; Shiao, H. Y.; Rafi, S.; Wang, S. Y.; Hsu, H.; Chen, C. H.; Chang, C. Y.; Chang, T. Y.; Lien, T. W.; Fang, M. Y.; Yeh, K. C.; Chen, C. P.; Yeh, T. K.; Hsieh, S. H.; Hsu, J. T.; Liao, C. C.; Chao, Y. S.; Hsieh, H. P. Design and synthesis of tetrahydropyridothieno[2,3-d]pyrimidine scaffold based epidermal growth factor receptor (EGFR) kinase inhibitors: the role of side chain chirality and Michael acceptor group for maximal potency. *J. Med. Chem.* **2010**, *53*, 7316–7326.

(30) Ishikawa, T.; Seto, M.; Banno, H.; Kawakita, Y.; Oorui, M.; Taniguchi, T.; Ohta, Y.; Tamura, T.; Nakayama, A.; Miki, H.; Kamiguchi, H.; Tanaka, T.; Habuka, N.; Sogabe, S.; Yano, J.; Aertgeerts, K.; Kamiyama, K. Design and synthesis of novel human epidermal growth factor receptor 2 (HER2)/epidermal growth factor receptor (EGFR) dual inhibitors bearing a pyrrolo[3,2-d]pyrimidine scaffold. *J. Med. Chem.* **2011**, *54*, 8030–8050.

(31) Jones, G.; Willett, P.; Glen, R. C.; Leach, A. R.; Taylor, R. Development and validation of a genetic algorithm for flexible docking. *J. Mol. Biol.* **1997**, *267*, 727–748.

(32) Yun, C. H.; Boggon, T. J.; Li, Y.; Woo, M. S.; Greulich, H.; Meyerson, M.; Eck, M. J. Structures of lung cancer-derived EGFR mutants and inhibitor complexes: mechanism of activation and insights into differential inhibitor sensitivity. *Cancer Cell* **2007**, *11*, 217–227.